JOURNAL REVIEW

Mixing in Continuous Crystallizers

The review is concerned primarily with some aspects of mixing in continuous crystallizers and recognizes the central importance of the interplay between the mixing and crystallization (or precipitation) processes in the design and performance evaluation of industrial crystallizers. The paper adopts a unifying treatment from a chemical reaction engineering viewpoint in which the Lagrangian approach to mixing in crystallizer systems is emphasized. The concepts of macro- and micromixing applied to crystallization configurations have been introduced with due emphasis on the modeling efforts. The present state of knowledge in various related areas of continuous mixing is assessed to help direct future trends in research.

N. S. Tavare
Department of Chemical Engineering
University of Manchester Institute of
Science and Technology
Manchester, M60 1QD, England

SCOPE

In recent years notable progress has been achieved in applying formalized unifying chemical reaction engineering principles to the analysis, simulation, and design of crystallizer configurations, but one significant gap in our understanding of crystallization processes is their interaction with mixing process. Using an analogy with the mixing description conventionally used in chemical reactors, this paper attempts to formalize the interplay between mixing and crystallization from the Lagrangian perspective. The mixing process is generally characterized by two distinct and independent elements, macro- and micromixing. The objectives of this review are to report the present state of the art and to direct further work on the characterization of mixing and its effects on the overall performance in conventional crystallizer configurations. Such a review may help in evaluating some of the research trends in this field.

CONCLUSIONS AND SIGNIFICANCE

The present article attempts a comprehensive treatment of mixing in continuous crystallizers from the Lagrangian perspective and has resulted in a recognized and straightforward chemical reaction engineering approach to the analysis of crystallization processes. The first part of the review deals with macromixing aspects, which covers major developments in analysis of residence time and crystal size distributions (RTD and CSD) with particular reference to modeling work. Clearly, CSD modeling is and will remain a popular and central topic of crystallization research. Both RTD and CSD studies should become more detailed and widespread for their greater engineering utility in the design, performance evaluation, and control of industrial units.

The second part of the review highlights the relatively new and important area of micromixing, i.e., mixing at the molecular scale. A small number of process simulation studies at extreme levels of micromixing have clearly demonstrated the enormous effects of the micromixing level on overall crystallizer performance. This may provide a comparatively sensitive and useful indicator of intermediate levels of micromixing. Characterization of real vessels of crystallization systems with complex nonlinear kinetic events is of paramount importance from both a theoretical and a practical viewpoint. Several types of *micromixing* models that have appeared in the chemical reaction engineering literature have therefore been reviewed to judge their applicability to crystallizer configurations.

Introduction

Crystallization is one of the important unit operations and is widely used in the chemical industry for a purification, separation, and/or production step for good quality crystals. The design, analysis, and simulation of crystallizers are of unique and prime interest to chemical engineers. Yet the systematic study of crystallizers is comparatively new in spite of crystallization's being one of the oldest unit operations used in industry. This slow development stemmed from a lack of understanding of the intrusion of complex physical phenomena on rate processes occurring in a multiphase, multicomponent system. Over the past three decades enormous advances in chemical engineering science, which evolved from the concept of unit operations via the more basic approach of transport phenomena, have paved the way in analysis and performance evaluation of crystallizer configurations.

In a rational approach to crystallizer design a solution of the relevant conservation equations representing crystal population and mass and energy balances, together with a description of the kinetics of rate processes involved and definition of flow patterns within the vessels, needs to be used. The performance of a crystallizer system depends not only on the pertinent intrinsic kinetics of growth and nucleation processes but also on the physical processes occurring in the vessel. The physical processes such as interphase and interparticle mass and heat transfer occurring within a multiphase crystallizer configuration depend very significantly upon the mixing characteristics of the phases involved.

By analogy with the conventional description of the mixing phenomenon in chemical reactors, the mixing process in crystallizers may be divided into separate contributions of two distinct mechanisms: macromixing (i.e., the residence time distribution, RTD), which defines retention times of the elementary volumes, and micromixing (i.e., mixing at the molecular level), which describes the communication between elementary volumes. These two contributions are independent of each other in that definition of a state of macromixing does not define a corresponding level of micromixing. As the names imply, the obvious difference between micro- and macromixing is in the scale of mixing that each describes. Micromixing generally includes all aspects of mixing not defined by the RTD. Each elementary volume or clump of the fluid in a vessel has a certain age and residual life. During a process a transition from groupings of clumps with identical ages to a grouping of clumps with identical residual life occurs, and this transition is characterized by the phenomenon of micromixing.

The Lagrangian perspective is used here primarily to describe mixing in a turbulent transport process. In such a description the changes of the property occurring to the elementary volumes or clumps are observed as a function of time as they progress through the vessel. In a Eulerian analysis the property variation is observed at a fixed point in a stationary coordinate system. It is important to note that in the Lagrangian system the average fluctuation of a characteristic velocity is the root mean square velocity fluctuation of many particles averaged along their respective particle paths; it is not a time average at a point in space as for the Eulerian system.

The scale of the segregation is a measure of the size of the unmixed clumps of the components, and as the clumps are reduced in size the scale of mixing is reduced. The intensity of segregation describes the effect of molecular diffusion on the mixing process. It is a measure of the difference in the concentration between the neighboring clumps of fluid. Gross fluid motion reduces the scale over which the differences exist, while diffusion reduces the intensity of the differences. Further fluid particles in a flow system have an attribute other than compositional which can be used to characterize the mixing. This attribute is called age and is the time that the fluid element, molecule, Brownian particle, or any other conserved entity has spent in the system. Characterization of mixing in terms of ages allows a unified and elegant treatment of continuous-flow systems that is independent of specific mixing mechanisms. This treatment is called residence time distribution theory and is the primary topic of the next section.

Macromixing

Residence time distribution

The concept of RTD is undoubtedly one of the most important of the ideas used in chemical reaction engineering to simplify complex situations in process vessels and to make them amenable first to analysis and ultimately to design. It was evolved from Danckwerts' fundamental insight (1953) and is based on a macroscopic lumped population balance description. It shows both theoretical elegance and practical utility in reducing the complexities of the physical situations for flow and mixing to a tractable form without discarding their essential complex features. Historically, RTD analysis has played an important role in process modeling, as evidenced by the abundance of literature on the subject over the past three decades. The basic concepts of RTD theory are quite simple and in most cases follow directly from elementary probability theory.

Any conserved entity such as a molecule, Brownian particle, elementary volume of fluid, or clump may be represented by the term particle. Particles enter the system, for example, a steady-state, continuous-flow vessel; remain in it for some period of time, which may be either deterministic or probabilistic; and eventually leave. In a general case a particle may make a number of temporary exits, with subsequent reentrances, but it is required that each particle have some original, first entrance and ultimate, final exit. Particles have zero age when they first enter and they acquire age at a rate equal to time spent within the system boundaries. The age of a particle at its last exit from the system is called the residence time of the particle. The residence time in general is a stochastic variable subject to a probability distribution. The normalized density function representing the distribution of the residence times of the particles leaving the vessel is called the dimensionless exit age distribution E or the RTD. The interrelations among the residence time distribution, E, cumulative RTD, F, internal age distribution, I, and (residual life) intensity function, Λ, are given in Table 1.

In the absence of complete knowledge of the flow and mixing within the vessel, an alternative approach of gaining partial information about how long the individual particles stay in the vessel has been adopted in RTD analysis. Such information, not sufficient to define completely the flow configuration, is relatively simple to obtain experimentally and can be interpreted easily. The experimental technique used for finding the desired RTD of particles in the vessel is a stimulus-response technique using tracer material in the flow. The stimulus or input signal is simply tracer introduced in a known manner into the feed stream entering the test section of the vessel. The input signal may be of any type, pulse, step, or periodic injections being the

Table 1. Relations Between the Dimensionless Age Distribution Functions

$$E(\theta) = \dot{F}(\theta) = -\dot{I}(\theta) = \Lambda(\theta)\exp\left[-\int_0^\theta \Lambda(\theta)\,d\theta\right]$$

$$\int_0^\theta E(\theta)\,d\theta = F(\theta) = 1 - I(\theta) = 1 - \exp\left[-\int_0^\theta \Lambda(\theta)\,d\theta\right]$$

$$\int_\theta^\infty E(\theta)\,d\theta = 1 - F(\theta) = I(\theta) = \exp\left[-\int_0^\theta \Lambda(\theta)\,d\theta\right]$$

$$\frac{E(\theta)}{\int_\theta^\infty E(\theta)\,d\theta} = -\frac{d\ln[1-F(\theta)]}{d\theta} = -\frac{d\ln[I(\theta)]}{d\theta} = \Lambda(\theta)$$

most common. The response or output signal is then the recording of tracer leaving the test section of the vessel. The system itself is at steady state when the tracer is injected. If the amount of tracer is small and does not alter the flow behavior of the system, then even though the tracer concentration varies with time in the system the basic steady state flow behavior of the system itself is not changed. It is assumed that the changes occurring within flow take place over time scales much shorter than those associated with the macroscopic dynamics of the system. Implicit in the assumption of steady state is that the residence time probability of a particle in the system is independent of the time of introduction into a system that exhibits both stationarity and ergodicity.

An RTD tracer study can yield important information on the linear physical processes occurring within the system, specifically the patterns of flow and degree of mixing among the particles that entered the system at different times. Comparison of RTD in vessels of the same type but different sizes gives an indication of the effect of scale-up on flow properties. The stimulus-response information is important in predicting the performance of equipment as long as the rate for a process is linear in an intensive property of a particle. For the proper modeling of the performance of multiphase process configurations, the RTD's of the various phases involved are of vital importance.

The single most important use for RTD studies is to determine a mathematical model of a system that represents the behavior of flow and mixing realistically enough to yield useful information for system design and analysis. The approach generally taken is to postulate a reasonable flow model on the basis of experimental tracer studies of the system and to correlate the model parameters with system properties so that the model output and actual response match as closely as possible. Naturally the closeness of the predicted response to actual tracer response curve will depend on how well the model mirrors reality.

By analogy with chemical reactors, the simplest crystallizer flow models from the liquid phase are the plug flow and the complete mixing flow models, which represent the two extremes of macromixing. Although no actual crystallizers can be fully represented by these idealized flow patterns, a number of crystallizers behave so closely to ideal that these models may be adopted with negligible error. At one extreme the liquid flow pattern in a crystallizer may be regarded as a plug flow with no longitudinal mixing but with complete radial mixing. This is characterized by an identical velocity and residence time of all particles within the crystallizer. For example, the flow pattern in a Kenics static mixer may perhaps be approximated by plug flow under turbulent flow conditions. (Randolph and Rivera, 1978). The other extreme is a completely mixed flow characterized by a well-defined RTD of exponentially decaying function and having identical composition properties in the exit stream and in the vessel contents within the crystallizer. The behavior of many vigorously stirred tank crystallizers may closely approximate this flow model.

A majority of actual crystallizer systems exhibit macromixing behavior somewhere between the two extremes of plug flow and ideally mixed flow, the residence time and residual life intensity functions of which are shown in Figure 1. The deviation from these two extreme cases may be caused by:

- Nonuniform liquid velocity profile
- Velocity fluctuation due to molecular or turbulent diffusion
- Short circuiting, bypassing and channeling of suspension
- The presence of stagnant regions of fluid caused by the crystallizer shape and internals
- Recycling of magma within the crystallizer as a result of agitation.

The actual crystallizer system perhaps may exhibit behavior more closely approaching the other curves of Figure 1.

Tracer tests of a system are useful in analyzing nonideality in flow patterns and the degree of mixing among elements that entered the system. When the flow behavior of the vessel is close to plug flow, the E curve would be almost symmetrical about the mean ($\theta = 1$ in this case) without any excessively long tail, while the Λ curve would be increasing, usually rather strongly. The spread of both curves about the mean would in general increase with the degree of mixing or the deviation from plug flow behav-

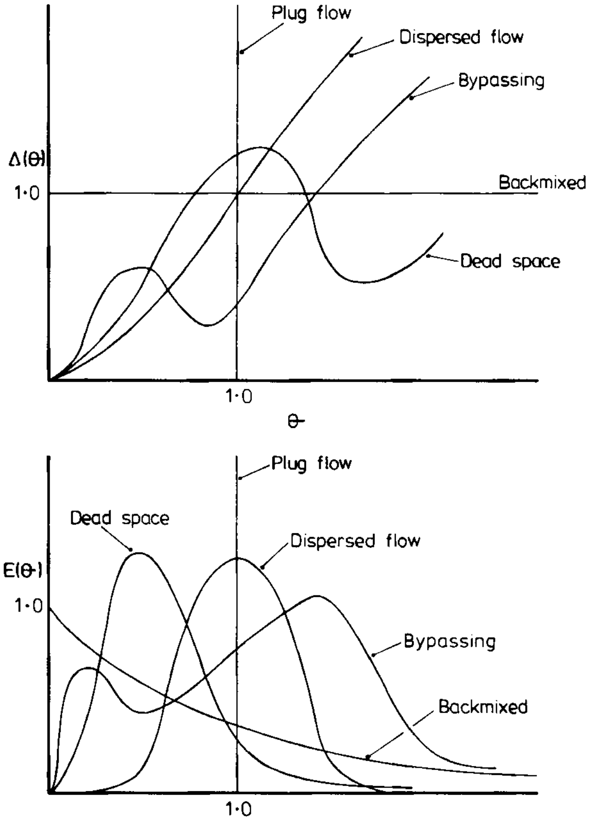

Figure 1. Schematic representation of characteristic response curves.

ior. The existence of dead space, i.e., a region in which fluid resides for times considerably longer than the overall mean residence time of the fluid actually flowing through the system, can be verified from the characterization of the E curve as indicated in Figure 1. The E curve will have a very long tail, indicating that fluid entering the dead space leaves only very slowly. The calculated mean of the E curve with the usual cutoff point (at $\theta \sim 3$) may be appreciably less than the true mean (i.e., unity). Bypassing refers to a condition in which some fluid elements pass through the vessel much more rapidly than others; i.e., a fraction of the fluid spends a time considerably shorter than the overall mean residence time of the fluid. If there is large dead space or significant bypassing, the distinction between the two is not clear-cut but depends on which part of the fluid is considered as a major part. The Λ can be used to identify the stagnancy, and it provides a measure of the dead space and/or bypassing of a system. Any particle that has resided in the system slightly shorter than the average first-part residence time has a high escape probability. However a particle that has remained in the system for a time longer than the first residence time has a high chance of being in the stagnant region and a lower probability of immediate escape. Thus, for dead space the Λ curve should have a decreasing portion somewhere past the vicinity of the average residence time ($\theta = 1$) and should increase again at long time when eventually all fluid leaves. For short times the small amount of bypassing fluid has an increasing Λ. After this fluid leaves, the remaining fluid will have a low probability until θ approaches the vicinity of unity, when Λ will increase again. The real utility of Λ is to determine the existence of the dead space from the experimental data, as the Λ curve has time-scale invariant shape characteristics and is sensitive to different flow conditions. For large amounts of dead space or bypassing, the two effects are not distinct. However, the equipment will not be allowed to run because of poor performance under those circumstances.

The Laplace transform of E has often been used as a characteristic function. Many manipulations turn out to be simpler with the Laplace domain representation $\overline{E}$ than with the time domain representation E. $\overline{E}$, the Laplace transform of E, serves usefully as a moment-generating function as

$$\mu_j = (-1)^j \left.\frac{\partial^j \overline{E}}{\partial p^j}\right|_{p=0} \tag{1}$$

When a process is governed by linear equations the Laplace transform can be used to obtain E, and if only the moments are required for the parameter characterization, a difficult inversion of $\overline{E}$ may often be avoided (Seinfeld and Lapidus, 1974). Quite often the response, $H(\theta)$, of the system to an arbitrary input, $Q(\theta)$, may be related to the RTD, $E(\theta)$, by the convolution integral as

$$H(\theta) = \int_o^\theta Q(\theta')E(\theta - \theta')d\theta' = \int_o^\theta Q(\theta - \theta')E(\theta')d\theta' \tag{2}$$

and the Laplace transform of a convolution integral is the product of the Laplace transforms of the functions involved. Thus

$$\overline{H}(p) = \overline{Q}(p)\overline{E}(p) \tag{3}$$

The Laplace domain formulation is useful in finding the composite density function for complex flow networks having statistically independent subsystems.

Flow models

Many types of flow models have been proposed to characterize nonideal flow within the vessel. Again by analogy with chemical reactors, homogeneous flow models for the liquid phase in crystallizers may be classified:

1. Velocity profile model, for a crystallizer whose velocity profile is rather simple and describable by a mathematical expression.
2. Dispersion model, which draws an analogy between mixing and diffusion and is a superimposition of diffusion on plug flow.
3. Compartmental model, which consists of a series of n-perfect mixing compartments.
4. Mixed model, which combines mixing, short-circuiting, and plug flow in various arrangements.
5. Circulation model, which considers various types of fluid motions within the crystallizer.

Once the data for the RTD are obtained, the backmixing characteristics for liquid of a crystallizer may be quantitatively evaluated by fitting appropriate models to these data. Models may vary in complexity. A simple one-parameter model may be quite adequate in some instances, but a much more refined and elaborate multiparameter model may be necessary in another circumstance. Some models are useful in accounting for the deviation of real stirred tanks from ideal mixed flow, others describe the deviation of real systems such as tubular vessels from plug flow, and still others may attempt to account for other contacting devices. Table 2 is the very roughest outline of the modeling efforts on the liquid phase in the crystallizers. For proper modeling of the performance of a multiphase crystallizer, RTD's of all phases are of vital importance, and the distribution of the solid phase produced needs to be considered.

The so-called stimulus-response technique involving tracer experiments is well-known in the RTD analysis of chemical reactors (see, e.g., Wen and Fan, 1975; Shah, 1979). Published information about the RTD analysis of the liquid phase in a crystallizer is relatively scanty. Grootscholten et al. (1981, 1982) attempted to characterize the RTD behavior of the main evaporative body of a salt crystallizer by measuring the tracer concentration response at the outlet for a step change in the circulating flow at the inlet. Saturated brine was used as a tracer in water at boiling temperature, circulated through the system, and detected continuously by conductometers. Using the RTD information the investigators could formulate a network model of liquid flow in the crystallizer involving a closed loop of ideal reactor units. Misztal et al. (1980) used the radioactive isotope of colloidal gold in the high-pressure and high-temperature crystallization of magnesium sulfate, for separation from low-concentration water solutions, to determine the RTD characteristics. The tracer adsorbs completely on crystals of magnesium sulfate and was detected after entry at two positions—in the liquid and solid phase, respectively. Two signals received from the probes were then used to determine the liquid-phase mixing characteristics based on the dispersion model. Identical RTD's for both the phases were tacitly assumed.

Table 2. Homogeneous Flow Models Used in Crystallizers

Model	References	
1. Velocity profile	Juzaszek and Larson	(1977)
	Randolph and Rivera	(1978)
2. Dispersion	Skrivanek et al.	(1967)
	Randolph and White	(1977)
	Randolph and Rivera	(1978)
	Misztal et al.	(1980)
	Grootscholten	(1982)
	Ring	(1984)
	Tavare	(1985a)
3. Compartmental	McCabe	(1929)
	Roberts and Robinson	(1957)
	Randolph	(1962, 1965)
	Nyvlt and Moudry	(1965)
	Nyvlt	(1971)
	Randolph and Larson	(1971)
	Abegg and Balkrishnan	(1971)
	Wolff and Larson	(1971)
	Tavare and Chivate	(1982)
4. Mixed	Bransom	(1965)
	Becker and Larson	(1969)
	Nyvlt	(1969, 1971)
	Nyvlt and Mullin	(1970)
	Randolph and Larson	(1971)
	Ramshaw and Parker	(1973)
	Grootscholten et al.	(1981, 1982)
5. Circulation	Wolff and Larson	(1971)
	Randolph and Tan	(1979)
	Nyvlt and Broul	(1979)
	Tavare et al.	(1985b)

Crystal size distribution

Randolph and Larson (1971) recognized the central importance of crystal size distribution (CSD) in the design and performance of industrial crystallizers, and provided as a unifying theme the interrelationships between the CSD on the one hand and crystallizer design criteria and operating problems on the other hand. Since then CSD studies have been appreciated by many researchers in the field and have become a central part of crystallization research. The study of CSD in crystallizers of any process configuration is in essence a study of the mean retention probability of individual particles as a function of their size and hence age. The authors introduced the term MSMPR (mixed-suspension, mixed-product removal) crystallizer to represent the ideally mixed flow configuration. This crystallizer behaves as though it were perfectly mixed; i.e., in any arbitrarily small element of volume, regardless of its location in the mixed section of the crystallizer, a full and uniform particle size continuum is assumed to exist. Further, such a crystallizer has unclassified product withdrawal, indicating that the same CSD exists in the product slurry and the crystallizer contents. The steady state CSD from a continuous MSMPR cyrstallizer having clear feed and negligible breakage or agglomeration is given by the solution of the dimensionless population balance equation

$$\frac{dyg}{dx} + y = 0 \tag{4}$$

as

$$y = \frac{yg|_o}{g} \exp\left[-\int_o^x \frac{dx}{g}\right] \tag{5}$$

where g may be a function of x as described in Table 3.

For a size-independent growth rate the dimensionless population density function from Eq. 5 can be derived as

$$y = \exp(-x) \tag{6}$$

or its equivalent in dimensional form as

$$n = n^o \exp(-L/G\tau) = \frac{B}{G} \exp(-L/G\tau) \tag{7}$$

Equation 7 represents the expected product CSD from an MSMPR crystallizer satisfying the above-mentioned assumptions and constraints. It contains two parameters, each being related to the system kinetics and constraints imposed. The parameter $G\tau$ is the product of the crystal growth rate and mean residence time of the system. The growth rate G is directly determined by the kinetics of growth and τ is the drawdown time, which is known in the operating system. The parameter n^o, the population density of nucleus size crystals, may be related to

Table 3. Size-Dependent and Dispersed Growth Rate Models

Growth Rate Model	Population Density	Reference
1. $g = 1$	$y = \exp(-x)$	—
2. $g = \alpha x^\beta$	$y = \frac{1}{g} \exp\left[\frac{-x^{1-\beta}}{\alpha(1-\beta)}\right]$	Bransom (1960)
3. $g = (1 + \alpha x)$	$y = (1 + \alpha x)^{-[(1+\alpha)/\alpha]}$	Canning and Randolph (1967)
4. $g = (1 + \alpha x)^\beta$	$y = \frac{1}{(1 + \alpha x)^\beta} \exp\left[\frac{1 - (1 + \alpha x)^{1-\beta}}{\alpha(1-\beta)}\right]$	Abegg et al. (1968)
5. Dispersed	$y = \frac{2}{1+\gamma} \exp\left[\frac{Pe}{2}(1-\gamma)x\right]$ where $\gamma = \sqrt{1 + 4/Pe}$	Randolph and White (1977) Tavare (1985a)

the kinetics of the nucleation and growth. These rates derive from the fundamental kinetic laws for nucleation and growth and the constraints imposed on the system, i.e., system parameters such as flow rate, vessel configuration, concentrations, and energy input or removal rate. In general, for a crystallizer operation the mass and energy flows are fixed from the process requirement, and the kinetics of nucleation and growth peculiar to the system determine the level of supersaturation and hence the growth rate that exists. The adjustable controls include the feed concentration, rate of energy input or removal, and feed rate.

In order to define fully the MSMPR configuration the mass balance also should be incorporated. Thus, for a continuous MSMPR crystallizer the rate at which the solute is depleted from the mother liquor must be equal to the rate at which mass is gained by the solid phase; i.e.,

$$c_i - c = M_T = 6k_v\rho_c B G^3 \tau^4 = \left(\frac{3k_v\rho_c}{k_a}\right) G\tau A_T \qquad (8)$$

Randolph and Larson (1971) have divided all the crystallization systems into two types for simplification in analysis. In class I systems the concentration drop across the crystallizer depends on the retention time and energy inputs; the system operates with measurable unrelieved supersaturation, and the yield depends on throughput. In class II systems the exit concentration approaches the saturation concentration at the working temperature and the per pass yield is independent of throughput. Equation 8 is valid at steady state for both class I and II systems.

By analogy with the intensity function (Naor and Shinnar, 1963) used in RTD analysis, Liu (1973) defined the crystal size intensity function (CSIF) such that $\Lambda(x)\,dx$ represents the conditional escape probability of crystals at size x within the next size increment dx in a specified unit of suspension. Figure 2 schematically represents the dimensionless population density and crystal size intensity function for a ubiquitous MSMPR crystallizer.

Although numerous techniques and theories have been devised to measure and analyze crystal growth, and to a lesser extent nucleation kinetics, the MSMPR crystallizer technique with its simple exponentially decaying steady-state CSD as represented by Eq. 7 has proved the most popular means of quantitatively measuring the growth and apparent nucleation rates, Figure 2. Analysis of experimental results is simple, and the technique has been used by many investigators (Shah and Garside, 1980). The steady state operation of a continuous crystallizer in an MSMPR mode requires not only complete homogeneity in suspension, but also isokinetic withdrawal of slurry. Although empirical correlations exist to predict the minimum speed for just suspending the crystals (Zwietering, 1958; Chapman et al., 1983) there exists no theoretical or empirical correlation in the literature that needs to be satisfied for achieving complete homogeneity in suspension.

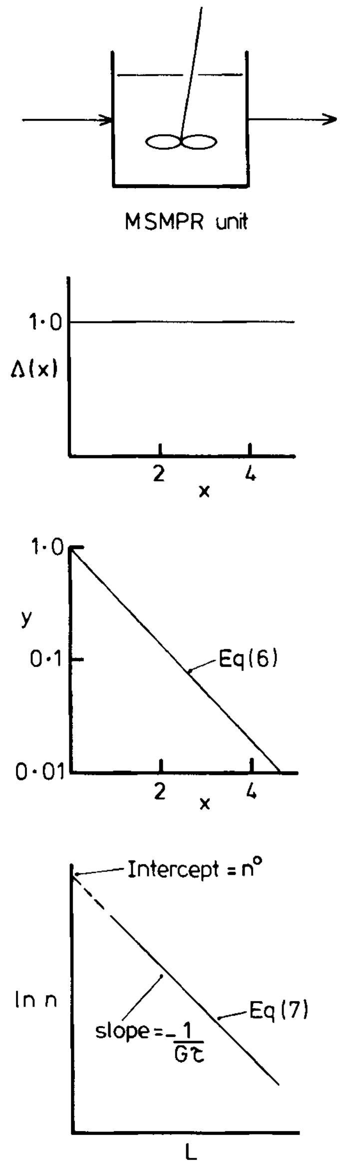

Figure 2. Schematic representation of characteristic curves for an MSMPR crystallizer.

Washout experiments may perhaps be useful to evaluate the macromixing performance of suspension in the vessel. In such experiments identical operating conditions are generally maintained in the vessels, and the crystallizer is fed with a saturated solution at the operating temperature. If an arbitrary impulse of distributed solid is charged into the continuously operated stirred-tank crystallizer, the concentration of the solid over all the crystal sizes is

$$M_i = \int_0^\infty k_v \rho_c n_i L^3 \, dL \qquad (9)$$

The exit concentration of the solid over the size range L and $L + dL$ for a perfectly mixed vessel to a delta input is the solution of the differential equation

$$-\frac{dM(L)}{dt} = \frac{M(L)}{\tau} \qquad (10)$$

and so is given by

$$M(L) = M_i(L) \exp(-t/\tau) \qquad (11)$$

where $M_i(L)$ is the equivalent initial concentration of the impulse. The overall solid concentration response, however, may be obtained by integrating Eq. 11 over all the size range to give

$$M = M_i \exp(-t/\tau) \tag{12}$$

The foregoing analysis indicates that not only the overall solid concentration but also a specific solid concentration at any size over a small size range should decay exponentially with time, having the same characteristic time constant for an MSMPR type crystallizer. Equation 11 is a relatively more stringent condition to achieve in practice.

Aeschbach and Bourne (1972) investigated empirically the hydrodynamic problem of achieving homogeneous suspensions and representative product withdrawal from a stirred tank configuration and suggested that constant tip speed may be a relevant scale-up criterion for homogeneous suspension. Zacek et al. (1982) reported a rapid washout test in a mini-MSMPR crystallizer using two sieve-size fractions. Results from the washout test may also provide some description of size-classifying action in the existing process configuration. Lieb (1973) attempted to characterize the perfect mixing representation in a randomly mixed suspension by using the condition of equal statistical marginal and conditional probability distribution of the crystal size. Grootscholten (1982) conducted elegant washout experiments at the end of the experimental run on a pilot crystallizer by operating it with a saturated brine at the operating temperature, and used the results to characterize the classification function. Alternatively, the comparison between the representative CSD's from the crystallizer contents and the product may perhaps provide similar information. It may be rather difficult and perhaps expensive to achieve true MSMPR conditions for a large industrial vessel. An MSMPR crystallizer produces product with wide distribution.

Formalization of the population balance approach to CSD modeling in continuous crystallizers led to an immediate burst of activity that entailed a systematic relaxation of constraints and assumptions used in an MSMPR configuration in order to delineate the observed CSD and also to improve the crystallizer performance.

Size-dependent growth rate

One of the early approaches used to interpret the nonlinear behavior of observed product CSD on the usual population density plot, particularly in the smaller size range, was to incorporate an empirical size-dependent growth rate expression in the population balance equations. Much of early experimental growth rate data has been correlated in terms of size-dependent growth rate models (Bransom, 1960; Garside et al., 1974; White et al., 1971; Garside and Jancic, 1978; Tavare and Chivate, 1979). Several size-dependent growth rate models have been proposed (Bransom, 1960; Canning and Randolph, 1967; Abegg et al., 1968) for use in combination with population balance equations in CSD modeling. Some of these models and the corresponding predicted dimensionless density functions in an MSMPR crystallizer are reported in Table 3. A typical set of dimensionless population density plots and corresponding dimensionless crystal size intensity functions are depicted in Figure 3. All the size-dependent models provide simple mathematical analysis without any mechanistic implication. For various parameter choices, all of the growth rate models listed in Table 3 predict growth rates either increasing or decreasing monotonically with size; the former predicts a wider distribution while the latter predicts a narrower distribution compared to the size-independent case. These effects show up as concave upward or concave downward curvature on the usual population density plot, but it is virtually impossible to distinguish such behavior from similar effects caused by size-dependent product removal.

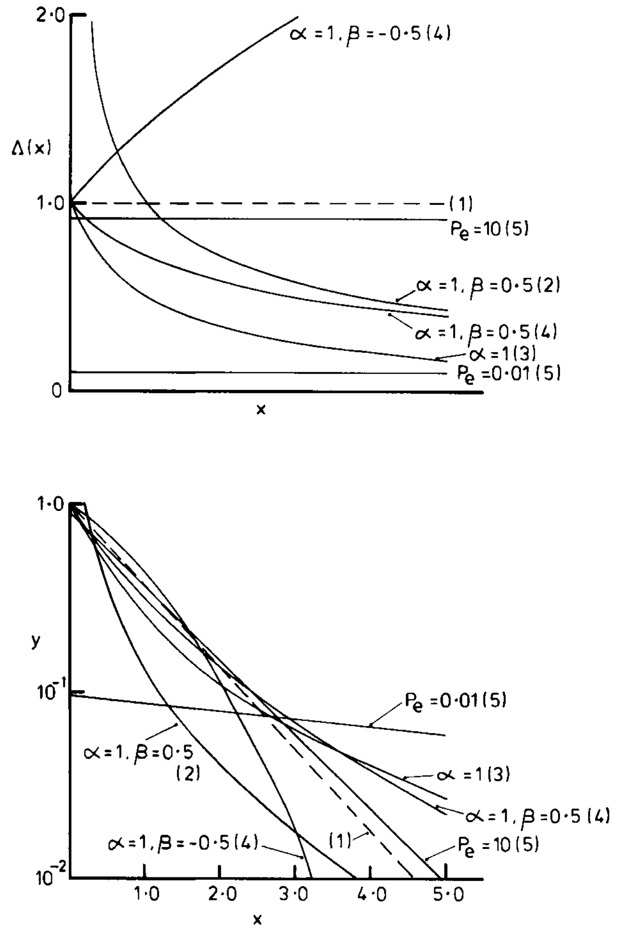

Figure 3. Growth rate models (Table 3).

Garside et al. (1976) pointed out that both the Gibbs-Thomson effect and the influence of bulk diffusion to the crystal surface are unlikely to be important in observed size-dependent growth kinetics, and suggested that perhaps the integration processes taking place at the crystal surface may induce the observed behavior. The size-dependent models have one or more adjustable parameters in order to represent the observed nonlinear population density plot. Such an empirical description will not have any ability to discriminate among the several causes.

Growth rate dispersion

In order to characterize the magnitude of the growth rate dispersion phenomenon, Janse and de Jong (1976) assumed that the growth rate is an independent property of a crystal, as each crystal grows at its own constant intrinsic growth rate throughout its life-span in an environment. They defined a two-dimensional modified population density function characterized by two independent variables, namely, crystal size and growth rate. Such an approach should add an additional dimension to the number-conservation equation and require an additional constraint to define the system. Usually the growth rate dispersion in the form of a statistical distribution (e.g., by gamma distribution) has been arbitrarily used (Janse and de Jong, 1976; Larson, et al., 1982; Berglund and Larson, 1984). Such two-dimensional models enormously complicate the CSD modeling and characterization of growth rate dispersion.

Randolph and White (1977) in their modeling of growth behavior for a crystallization system pointed out the close analogy between growth rate dispersion and axial dispersion in chemical reactors. They added a second-order term to the population balance of an MSMPR crystallizer under steady state conditions and used two boundary conditions, representing the population flux at the entrance and the asymptotic bound on the population density. With this description they derived an exponential distribution with apparently a larger mean size than expected based on true mean growth rate and unchanged coefficient of variation. The true average growth rate may be either an externally manipulated or a constrained variable determined from solution of population and mass balances together with system kinetics. Solution of the dimensionless population balance with a set of boundary conditions for the steady state MSMPR crystallizer is also included in Table 3. Thus the wide exponential distribution of the MSMPR crystallizer as shown in Figure 3 is unaffected in form by addition of a growth dispersion term. The Peclet number for crystal growth characterizes the extent of dispersion. A higher value of Peclet number will indicate a lesser dispersion effect, and the dimensionless population density (case 5, Table 3) tends to approach an MSMPR solution (case 1, Table 3).

Inclusion of a size-dependent growth rate model in the description of an MSMPR crystallizer would in general add a nonlinear element in the population balance, whereas addition of a second-order term would be required for the dispersion effect. Although nothing is implied specifically concerning the actual mechanism, in both descriptions the experimental evidence tends to suggest that the surface integration processes appear to be important (Garside et al., 1976; Tavare and Garside, 1982a, b, c; Garside et al., 1984). Recently Ring (1984) used the CSD information obtained from continuous precipitation of titanium dioxide in a packed-bed crystallizer to characterize the vessel dispersion characteristics. Tavare (1985a) suggested that the transient tracer information from the solid phase in a continuous MSMPR crystallizer may perhaps help solve the characterization and/or discrimination between the two effects. In practice, it is quite likely that both growth rate dispersion and size-dependent growth may occur concurrently in a real system, which would further complicate the analysis.

Size-dependent residence time distribution

In certain commercial crystallizer designs, residence times of mother liquor and crystals are often separated to provide better yield and/or size improvement. Fines removal, classified product withdrawal, and double draw-off are three crystallizer configurations that utilize deliberate size-dependent removal rates to manipulate CSD. Randolph and Larson (1969, 1971) elegantly modeled those configurations with the so-called R-z crystallizer model, in which fines and product removal rates are respectively R and z times the MSMPR removal rate, and showed that these configurations can dramatically affect both the CSD and the level of supersaturation. In general, the accelerated fines removal configuration produces a larger product with a wider distribution, while accelerated classified product removal produces a narrower distribution of smaller size. The double drawoff configuration results in higher yield and perhaps some size improvement. The dimensionless population density for the R-z model over the three sections of the size range is

$$\begin{aligned} y &= \exp(-Rx); \quad 0 < x < x_F \\ &= \exp[-(R-1)x_F]\exp(-x); \quad x_F < x < x_C \\ &= \exp[-(R-1)x_F]\exp[(z-1)x_C]\exp(-zx); \quad x_C < x \end{aligned} \tag{13}$$

where x_F and x_C are fines removal size and classification size, respectively. The continuity in the CSD distribution, Eq. 13, is implicitly assumed. Both Juzaszek and Larson (1977) and Randolph and Kraljevich (1978) have demonstrated the experimental verification of the R-z crystallizer model. Randolph (1979) pointed out that the product CSD obtained from large-scale commercial crystallizers operating with fines destruction system to produce large particles for, e.g., ammonium sulfate and potassium chloride systems, agrees qualitatively with the model predictions.

In a classified product removal configuration the mean retention probability is dependent on the particle size. Removal of product crystals may be accelerated (decreased retention probability, i.e., $z > 1$) or retarded (increased retention probability, i.e., $z < 1$) relative to the MSMPR case, producing narrower or wider CSD than MSMPR product CSD. Elutriators, hydroclones, or wet screens may be used as classification devices. Inadvertent size classification can occur at the point of slurry removal in a mixed suspension. The idealized descriptions used above and by Saeman (1956), Randolph (1965), Nyvlt (1967), and Han and Shinnar (1968) utilize the point classification models.

Janse and de Jong (1976) and Bourne (1979), however, used a smooth, continuously varying function of crystal size in order to represent the gradual classification occurring in mechanically stirred tank crystallizers either because of poor hydrodynamic conditions in the vessel or nonisokinetic withdrawal at the slurry discharge. They defined the classification function as

$$\lambda(x) = \frac{n_p}{n_c} = \frac{\tau}{\tau(x)} \tag{14}$$

where $n_p dx$ is the number of product stream particles and is λ times the number of particles ($n_c dx$) in the well-mixed crystallizer over the dimensionless size x and $x + dx$. $\tau(x)$ is the size-dependent residence time of particles over the same size range. $\lambda(x)dx$ represents the escape probability of crystals over the size range x and $x + dx$, and thus $\lambda(x)$ is tantamount to the crystal size intensity function $\Lambda(x)$.

The $R - z$ crystallizer model can be simulated in terms of $\lambda(x)$ as

$$\begin{aligned} \lambda(x) &= R; \quad 0 < x < x_F \\ &= 1; \quad x_F < x < x_C \\ &= z; \quad x_C < x \end{aligned} \tag{15}$$

The CSIF, $\Lambda(x)$, Eq. 15, and corresponding dimensionless population density function, Eq. 13, are shown in Figure 4. The classification function for a particular vessel under a given set of

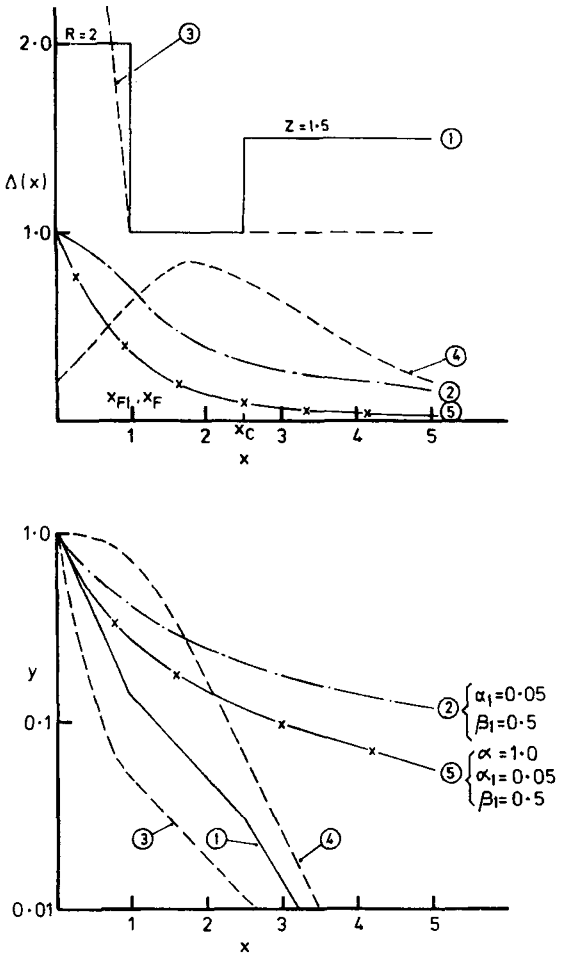

Figure 4. Size-dependent RTD models.

1. *R-z* model (Randolph and Larson, 1971
2. Continuous classification (Bourne and Zabelka, 1980)
3. External classification (Grootscholten, 1982)
4. Internal classification (Grootscholten, 1982)
5. Continuous classification and linear size-dependent growth (Bourne and Zabelka, 1980; Canning and Randolph, 1967)

operating conditions can be determined from washout tests (Bourne, 1979; Bourne and Zableka, 1980).

Some examples of experimental data showing various forms of size-dependent removal rates with their corresponding dimensionless population density functions are also included in Figure 4.

The second curve in Figure 4 corresponds to a situation where the larger crystals are preferentially retained as they have less escaping probability. Bourne and his co-workers (1979, 1980) used an empirical relation of the type

$$\lambda(x) = \frac{1 + \alpha_1 x^2}{1 + \beta_1 x^2} \tag{16}$$

in order to represent the gradual classification function characterizing the hydrodynamic state of the vessel, and derived an analytical solution for the population density as

$$y = \exp\left[-\frac{\alpha_1 x}{\beta_1} - \frac{(1 - \alpha_1/\beta_1)\tan^{-1}(\sqrt{\beta_1}\,x)}{\sqrt{\beta_1}}\right] \tag{17}$$

The third curve in Figure 4 represents schematically the case where crystals having a size smaller than a characteristic size (x_{F1}) are preferentially withdrawn in the product and have linearly decreasing escape probability with size. A similar classification function was observed at the product removal point by Grootscholten et al. (1981) in their 1.5 m^3 pilot-scale external forced-circulation salt crystallizer. The external classification for this case may be simulated as

$$\begin{aligned} \lambda(x) &= -\beta_2 x + \beta_2 x_{F1} + 1; \quad 0 < x < x_{F1} \\ &= 1; \quad x_{F1} < x \end{aligned} \tag{18}$$

where x_{F1} is a characteristic classification size of the model observed in the crystallizer configuration, and the corresponding population function may be derived as

$$\begin{aligned} y &= \exp\left[\beta_2 \frac{x^2}{2} - (\beta_2 x_{F1} + 1)x\right]; \quad 0 < x < x_{F1} \\ &= \exp\left[-\beta_2 \frac{x_{F1}^2}{2} - x\right]; \quad x_{F1} < x \end{aligned} \tag{19}$$

Grootscholten (1982) further characterized the internal classification in the evaporator body, and the fourth curve in Figure 4 represents schematically the observed internal classification function in his forced-circulation salt crystallizer. He speculated that the peculiar shape of the internal classification is due to the particle interaction in their settling behavior. The population density function for any classification function $\lambda(x)$ may be derived by

$$y = \exp\left[-\int_o^x \lambda(x)\,dx\right] \tag{20}$$

The integral in Eq. 20 may be evaluated numerically.

The fifth curve in Figure 4 represents the combined effect of both the gradual classification (as by Eq. 16) and size-dependent growth (as given by the Canning and Randolph, 1967, model—: case 3, Table 3). The population density function can be evaluated from

$$\begin{aligned} yg &= \exp\left[-\int_o^x \frac{\lambda(x)}{g(x)}\,dx\right] \\ &= \exp\left[-\int_o^x \frac{(1 + \alpha_1 x^2)dx}{(1 + \beta_1 x^2)(1 + \alpha x)}\right] \end{aligned} \tag{21}$$

Both the crystal size intensity function and the residence time intensity function help indicate the relative deviation from the ideal exponentially decaying distribution function. The crystal intensity function provides an explicit dependence of escaping probability of crystal particles on the particle size. Perhaps both $y(x)$ and $\Lambda(x)$ together give better representation of the possible mechanism leading to the deviation from the ideal cases. In general higher $\Lambda(x)$ shifts $y(x)$ toward down right, while lower $\Lambda(x)$ shifts it toward up left. (See, e.g., Figures 3 and 4.)

Agglomeration and breakage

In general, agglomeration and/or breakage should represent discontinuous particle trajectories in the particle phase space,

Table 4. Agglomeration and/or Breakage Studies

Investigators	Major Features
Smoluchowski (1916, 1917)	Particle collisions; two types of agglomerations: perikinetic (diffusion controlled collisions, static fluid, smaller size ($\sim 0.1\ \mu m$) colloidal particles moving by Brownian motion, second-order with particle concentration, temperature-dependent) and orthokinetic (shear controlled collisions, agitated dispersions, larger particles, first-order with particle concentration, size- and shear-dependent).
Hulburt and Katz (1964)	Inclusion of agglomeration term based on two-particle collision in population balance equation for plug flow type and batch crystallizers.
Walton (1967)	Qualitative characterization of agglomerating system with high particle concentration ($>10\%$ of the particles should agglomerate in $\sim 10^3 s$).
Randolph (1969)	Representation of two-body breakage in population balance by birth and death functions using idealized probability distributions like uniform, equal size, or attrition breakage distributions.
Rosen and Hulburt (1971)	Characterization of breakage for crystallization of potassium sulfate in a vacuum MSMPR crystallizer. The model assumes uniform breakage below a characteristic breakage size.
Wahl and Baker (1971)	Modeling of agglomeration of titanium dioxide pigment (0.2–1.0 μm) dispersed in an agitated isoton used as electrolyte, based on collision frequency due to turbulent motion, by sequential counting of particles with Coulter counter. Effect of particle concentration and stirring rate.
Maruscak et al. (1971)	Characterization of agglomeration in precipitation of calcium carbonate in CMSMPR precipitator.
Sakamoto et al. (1971)	Study of agglomeration during alumina precipitation.
Fitzgerald and Yang (1972)	Steady state CSD from an MSMPR crystallizer with growth and breakage; the breakage model assumes random breakage with identical probability and volume conservation.
Matusevich (1966) Holldroff et al. (1975)	Effect of hydrodynamics and operating conditions on agglomeration behavior during crystallization of potassium chloride and potassium nitrate.
Halfon and Kaliaguine (1976)	Characterization of both breakage and agglomeration from product CSD responses in precipitation of aluminium trioxide from caustic aluminate solution.
Liao and Hulburt (1976)	Evaluation of crystallization and agglomeration kinetics of potassium sulfate in an MSMPR crystallizer by using analytical solution to the agglomeration model based on two-particle collisions.
Remillard et al. (1978, 1980)	Modeling of agglomeration and attrition phenomena in crystallization of alumina trihydrate in an isothermal batch and CSTR.
Grabenbauer and Glatz (1981)	Modeling and characterizing of agglomeration, breakup, and growth processes for precipitation of soy protein at isoelectric point in an MSMPR crystallizer.
Groenweg and Hoffman (1981)	Numerical algorithm to solve population balance equation.
Schubert (1981)	A review on agglomeration dealing with fundamentals, practical aspects, and processes.
Kau and Torocheshikov (1982)	Theory of crystal aggregation in bulk crystallization from solution including the effects of particle break-up and mass transport based on mechanistic description.
Hoare (1982a,b)	Controlled precipitation and aging of protein precipitation by salting out of casein in a helical ribbon stirred reactor involves combined aggregation and shear break-up.
Kawashima et al. (1982)	Use of wet spherical agglomeration technique for the preparation of spherical wax matrices of sulfamethoxazole in an MSMPR agglomerator.
Petenate and Glatz (1983a,b)	Modeling of isoelectric precipitation of soy protein in an MSMPR precipitator to characterize the aggregate growth and breakage from the steady state CSD. Growth of aggregates by a turbulent collision and breakage by hydrodynamic shear mechanisms.
Twineham et al. (1984)	Shear induced breakup of isoelectric soya protein precipitate arises from particle collisions and is represented by a first order relationship for change in particle size with time.
Kawashima et al. (1984)	Effect of temperature on the production of spherically dense agglomerates of salicylic acid.
Tavare et al. (1985c)	Conventional kinetic expressions for crystallization and agglomeration for precipitation of nickel ammonium sulfate in an MSMPR crystallizer.
Grootscholten et al. (1985)	Characterization of breakage caused by fragmentation in different draft tube crystallizers for salt crystals is carried out in terms of birth and death functions in population balance equations.
Nyvlt and Karel (1985)	Assessment of agglomeration by three techniques: visual determination of percent agglomeration, numerical correction of CSD to find the degree of agglomeration, and the method of decomposition of the two-peak CSD.

and can formally be represented in the population balance by the birth and death functions. These functions should be formulated on the basis of empirical description of the state of a system. They should also preserve internal consistency; a birth event at one size represents one or more death events at some other size(s). Some generalizations and simplifications of these birth and death terms are however possible. Table 4 lists the studies relating to the characterization of agglomeration and/or breakage behavior of systems during the crystallization processes.

Although the precise mechanisms of both agglomeration and breakage are difficult to conceive, a simple mechanism based on two-body collisions has generally been used in formulating the rate models. Thus, both these phenomena may be approximated by a sequence of two-body death and birth events. If the form of any one (i.e., either birth or death) function is postulated as a function of the state of the system, a corresponding, consistent two-body other function can be constructed to represent the distribution at some other place(s). Once these birth and death functions are characterized, the population density may then be derived from the population balance equation. The agglomeration model proposed by Liao and Hulburt (1976) considers the formation of agglomerates due to two-particle collisions. Curve 1 in Figure 5 represents the dimensionless population density based on their analytical solution and corresponding intensity function. The second curve in Figure 5 corresponds to a breakage model suggested by Rosen and Hulburt (1971) which assumes that the shattering occurs below a critical breakage size at a uniform rate but zero above this size. The results show that breakage changes the CSD in a way very similar to product classification. Randolph (1969) identified three idealized models of a two-body breakage distribution, namely, attrition, uniform but random breakage, and equal size cleavage. Crystal attrition would not change the form of the distribution significantly, while the latter greatly affects product narrowness. Using a power law size-dependent, two-body, equal-size-breakage function with an exponent β_3 and a fraction of breakage relative to removal at MSMPR dominant size, m, the author showed that the size distribution was narrow and the population density plot was concave downward, as depicted by curve 3 in Figure 5. All these models use the characteristic length of the particle as an additive property. However, the conservation of mass (or volume) rather than the characteristic length is more appropriate in the modeling.

Neither agglomeration nor breakage may be of major importance in well-designed commercial crystallizers producing well-defined crystals. Heavy slurry densities and long retention times inevitably result in crystal attrition giving rounded crystal habit and increased apparent nucleation. Generally, morphologically ill-defined precipitates encounter both these phenomena, which may present severe problems for subsequent processing. Sometimes during pure agglomerate formation continuous growth may not occur, and the corresponding convective growth term in the model is then absent.

Multistage configurations

As the inherently simple MSMPR crystallizer yields a wide exponentially decaying product CSD, a multistage crystallizer configuration should show promise toward improving the product CSD because of its narrow RTD. Table 5 provides a good compilation of modeling efforts on multistage crystallizer configurations. Various strategies can be employed to alter the product CSD. Among these are conditions that permit nucleation in the first stage and only growth in the subsequent stages, and equal nucleation in each stage of a cascade of MSMPR crystallizers. However, it is more realistic to recognize that both nucleation and growth occur in each stage at rates determined by the prevailing operating conditions. The influence of the nucleation process on the product CSD is also important. Figure 6 compares the performance of product CSD obtainable from a five-stage cascade of MSMPR crystallizers. The broken-line curves give the variation of normalized growth and coefficient of variation of product weight distribution with stage number at different relative kinetic orders (Tavare and Chivate, 1982). Equal residence time and equal solid deposition were allocated in each stage of a five-stage cascade and normalized with respect to a single-stage MSMPR configuration. The solid curve A in Figure 6 represents the performance corresponding to a case having nucleation in the first stage, while curve B corresponds to a case of equal nucleation in each stage of a five-stage cascade (Abegg and Balkrishnan, 1971). Thus, if nucleation can be confined to the first stage alone, the cascade of MSMPR crystallizers may produce a narrower CSD.

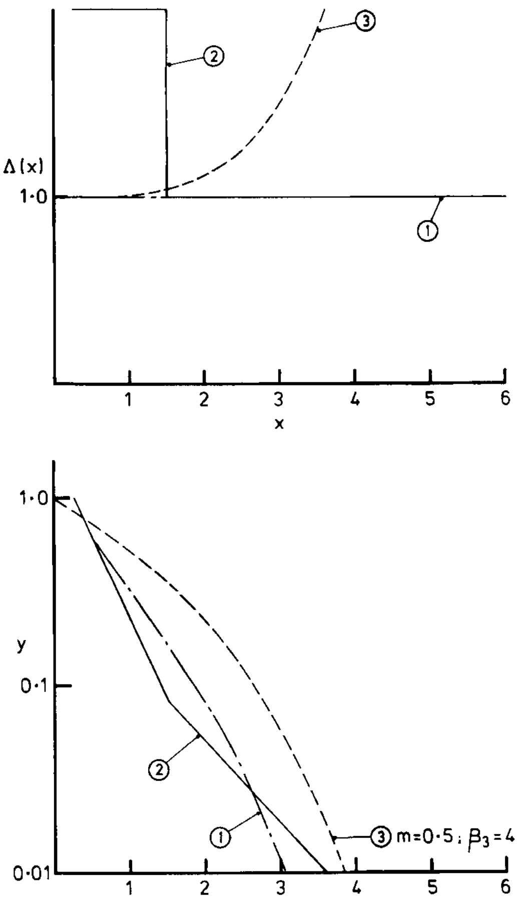

Figure 5. Agglomeration or breakage models.
1. Agglomeration (Liao and Hulburt, 1976)
2. Breakage (Rosen and Hulburt, 1971)
3. Breakage (Randolph, 1969)

External seeding is another process modification rarely used in commercial operation, with the exception of sucrose crystalli-

Table 5. Studies of Multistage Crystallizers

Investigators	Major Features
	MSMPR Crystallizers in Series
McCabe (1929)	Crystallization of gypsum in phosphoric acid manufacture.
Roberts and Robinson (1957)	Narrowing of product CSD, nucleation in first stage only.
Randolph (1962)	Possibility of bimodal weight distribution; equal nucleation, growth.
Randolph (1965)	Two-stage cascade with allocation of residence time and mass deposition.
Hill (1970)	Comparison between coefficient of variations obtained from cascade of MSMPR crystallizers and dispersed plug flow crystallizer.
Nyvlt (1971)	Optimal temperature distribution; concept of number of theoretical crystallizer units; equal and first-stage nucleation.
Randolph and Larson (1971)	A general CSD algorithm for various operating conditions.
Abegg and Balkrishnan (1971)	Mixing effects by tanks-in-series; equal and first stage nucleation.
Wolff and Larson (1971)	Cascade performance in relation to single stage; optimal allocation of resources.
Nyvlt et al. (1973)	Mixing effects by tanks in series; equal nucleation.
Terwillinger and Wey (1976)	First-stage nucleation; empirical determination of maximum permissible growth rate.
Rojkowski (1977)	Optimal allocation; temperature profile.
Skrivanek and Vacek (1977)	Evaluation of CSD moments in cascade having alternate growth and dissolution cells.
Nyvlt and Provaznik (1979)	Optimization of five-chamber crystallizer for Glauber salt.
Tavare and Chivate (1982)	Cascade performance in relation to single stage, optimal allocation; effect of relative kinetics, general CSD algorithm.
	MSCPR Crystallizers in Series
Randolph et al. (1965)	First-stage nucleation; narrowing of CSD.
Tavare and Chivate (1978)	Two-stage cascade performance in relation to single-stage, optimal relation of classification ratio and size.
Recycle	
Wolff and Larson (1971)	Restricted investigation of MSMPR cascade with recycle shows no benefit
Randolph and Tan (1978)	Simulation for staged classified recycle crystallizers for alumina and sugar.
Nyvlt and Broul (1979)	Recycle of mother liquor; effect of recycle on purity.
Tavare et al. (1985b)	Higher recycle ratio in MSMPR cascade with recycle configuration is important; mixing characterization.

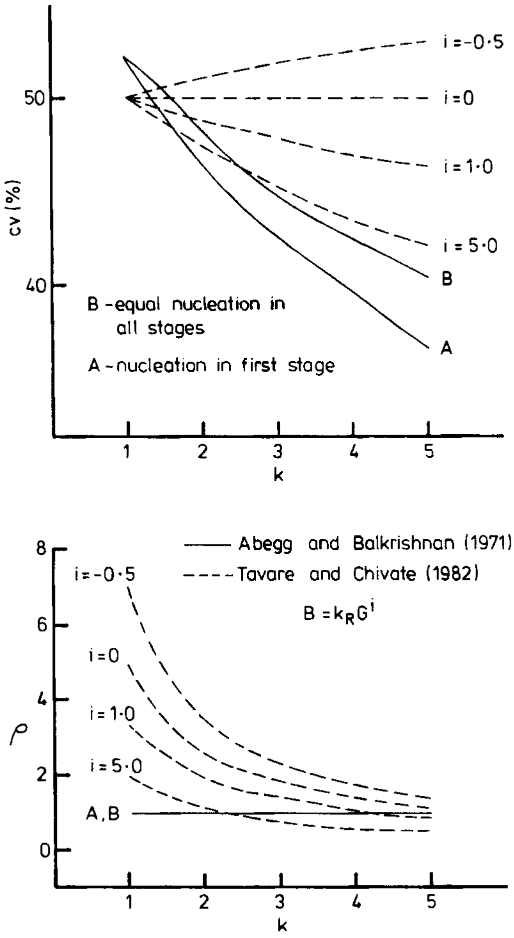

Figure 6. Effect of nucleation on product CSD in a cascade of MSMPR crystallizers.

zation. Broadfoot and White (1975) have modeled seeding in a cascade of MSMPR units for continuous sugar crystallization in order to achieve narrow product CSD.

General algorithms have been developed to calculate the performance measures of crystallizer cascades of various configurations, and even optimal specifications have been determined in order to achieve the best possible performance (see Table 5). Almost all the analyses with cascades of MSMPR and MSCPR crystallizers tend to suggest that under realistic practical conditions with a limited number of units in a configuration, only marginal improvement in product CSD can be realized and staging by itself is an inefficient way of improving the performance. However, certain chemicals requiring long residence time and large production capacity can be crystallized in a series of crystallizer bodies in order to restrict the vessel size to a manageable proportion and gain marginal size improvement.

Macromixing models

By analogy with chemical reactors, the tanks-in-series concept has been proposed as a mixing model by several investigators (see Table 5). The basic concept of this model is that of dividing an imperfectly mixed suspension into a number of sections of usually equal volumes, each of which is assumed to be perfectly mixed. Each section of the real suspension is then represented by a perfectly mixed crystallizer having the attributes of the section in question. Thus an imperfectly mixed crystal suspension is represented by a cascade of perfectly mixed crystallizers. If all the sections are assumed to have identical independent attributes, then the number of units in the cascade is the model parameter. Perhaps the most important use of analysis of multistage configurations is to calculate the type of product CSD's that can result when the crystallizer is not perfectly mixed and is simulated by tanks-in-series model. Nyvlt (1971) and his co-workers determined the number of theoretical crystallization units (NTCU) in an imperfectly mixed crystallizer using their analysis of cascade configurations. The concept was verified for experimental data obtained from laboratory crystallizers producing calcium nitrate, ferrous sulphate, and urea. Abegg and Balkrishnan (1971) have also used a similar tanks-in-series concept to characterize imperfectly mixed suspensions, using the data of Bennett (1962) from industrial-scale crystallizers and predicted NTCU for many systems. Both investigations have used the cases of either nucleation in the first stage alone or equal nucleation in all the stages. The analysis by Tavare (1978), however, suggests that the assumed nucleation characteristics have an important effect on the performance measures deduced for a cascade configuration.

In addition to the tanks-in-series concept described above, the other approach to representing nonideal flow behavior is to use the dispersion models, which draw on the analogy between the mixing in actual flow and a diffusional process. The dispersion or Peclet number based on the vessel characteristics is a model parameter that measures the extent of axial dispersion and characterizes the mixing state of the crystallization system (Randolph and White, 1977; Randolph and Rivera, 1978). Thus, a large value of Peclet number indicates negligible dispersion effects and the vessel tends to behave like a plug flow crystallizer. For a small value of Peclet number the crystallizer will show large dispersion effect and it will be more of the backmixed flow type.

By analogy with chemical reaction engineering, one-parameter models such as tanks-in-series and dispersed plug flow models may be ideally suited to account for the nonideality in flows that do not deviate greatly from their corresponding ideal flow patterns. However, when the flow patterns are very different from the ideal flow configuration, multiparameter models are likely to represent the configuration more satisfactorily. Many such multiparameter models have been suggested for chemical reactors and may perhaps be suitable to represent flow in real crystallizers. Relatively little work on multiparameter modeling is available in the crystallization literature. Becker and Larson (1969) used the mixed models approach, which assumes that the flow within the continuous vessel can be divided into various interconnected regions whose flow characteristics can be precisely described. In their idealized simulation they considered a system consisting of a plug flow section followed by a well-backmixed section, and showed for a case of second-order relative kinetics that the highest solid deposition is achieved in a system in which the backmixed portion occupies 18% of the total volume and the largest weight mean size 60% of the total volume. In order to interpret the peculiar shapes of the product CSD obtained from pilot plant units of salt crystallizer, Gootscholten et al. (1981, 1982) simulated the crystallizer as a closed loop of idealized sections of plug flow and backmixed flow on the basis of the RTD behavior of the vessel. Good agreement was observed between the experimental and simulated product CSD's. Tavare et al. (1985b) suggested a mixing model consti-

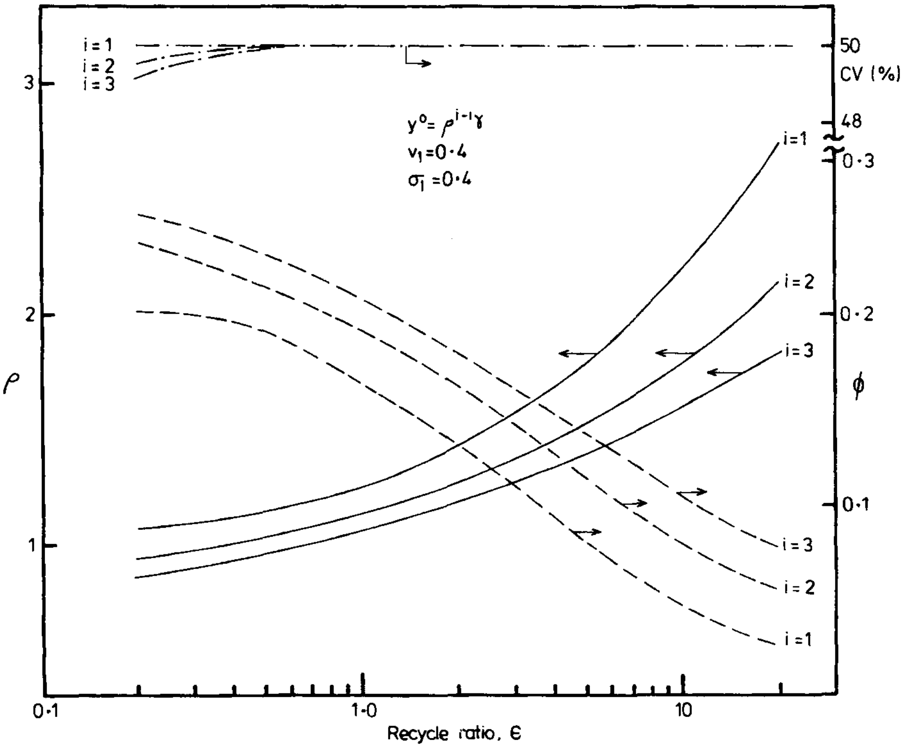

Figure 7. Performance characteristics of two-stage cascade of MSMPR crystallizers with magma recycle (Tavare et al., 1985b)

tuting a well-mixed tanks-in-series with magma recycle configuration where the number of stages in the cascade and recycle ratio were used as model parameters. The simulation of a large forced-circulation Oslo unit and an imperfectly mixed large precipitation vessel may perhaps be better represented by a two-stage cascade of MSMPR crystallizers with magma recycle process configuration. Figure 7 represents the statistics of the product CSD obtained with recycle ratio defined as ratio of product to recycle mass flow rate. The product mean size increases with recycle ratio for all relative kinetic orders, as the higher recycle ratio forces the system to operate at higher growth rate levels, and decreases with increasing relative kinetic order for all recycle ratios. At a higher recycle ratio for all relative kinetic orders the product CV is the same and equal to that of an MSMPR unit (50%). As the recycle ratio approaches zero the product CV approaches the value corresponding to that of a two-stage cascade of MSMPR crystallizers for a given relative kinetic order. The recycle ratio at its higher value becomes an important variable that governs the growth rate levels and maintains the MSMPR condition within the entire configuration.

CSD dynamics and control

Understanding CSD dynamics in commercial crystallizers with large holding time is sometimes important. Observation of CSD instability on an industrial scale provided the original impetus to formalize the population balance approach to dynamics modeling. CSD dynamics caused by a nonhomogeneous (outside) forcing function is referred to as CSD transients, and that caused by inherent instability of the characteristic equations describing CSD is referred to as CSD instability. The analyses of these two sources of CSD dynamics stems from the same dynamic population and mass balances coupled with the system kinetic events, but proceeds along different paths; the corrective actions required to stabilize the CSD are also different. Table 6 includes a list of studies relating to CSD dynamics and control. Much attention in the literature has been given to understanding the dynamics and stability of CSD. Control studies, however, are comparatively few in number. In typical industrial crystallization practice usually no attempt is made to control CSD transients other than to minimize the major system upsets. Undoubtedly, the lack of simple on-line system identification techniques based on either solution or solid-side information has inhibited the application and implementation of control schemes. Recent work by Randolph and his co-workers (Table 6) attempted to establish the feasibility of on-line measurement of fine crystal CSD in order to characterize growth and nucleation events and subsequently use them in the control scheme.

Micromixing

Limits of micromixing

The RTD approach by itself does not completely define a state of mixing and is concerned with macromixing, meaning those gross flow processes that cause different clumps to have different residence times. These same processes may or may not cause any mixing at a molecular level of scrutiny. Thus, if the individual clumps were encapsulated they could flow through the system and have a distribution of residence times without any mixing on the molecular scale. Such a system is said to be completely segregated (Danckwerts, 1958) and represents one limit on micromixing—the case where there is no micromixing at all within the vessel. In this mixing situation an element of suspension travels through the vessel in discrete, noninteracting packets or clumps that constitute the particles of RTD theory. The contents of the vessel behave as a macrofluid. The performance of the vessel in such a configuration is exactly as if each clump were a small batch crystallizer. They all have the same entering conditions but have different exit conditions depending on their residence times in the vessel. As the product at the vessel exit is assumed to be completely mixed, the average exit performance characteristics can be evaluated by summing over those of the myriad of batch crystallizers at the exit weighted with the normalized RTD function.

There is also the other limit, that which corresponds to the highest level of molecular mixing possible with a given RTD. This is called maximum mixedness (Zwietering, 1959). In this mixing situation the entering clump in the feed mixes immediately with material already in the vessel, loses its identity, and has no determinable past history. The vessel contents behave as a microfluid. The performance characteristics for the vessel are evaluated by the usual methods for continuous crystallizers.

In order to develop a computational tool for performance evaluation of the vessel in these extreme limits it is necessary to define a notional point in the sense used by Danckwerts (1958), and some additional time-coordinate properties of the continuous flow systems. A point is defined as an element of suspension, small compared to the total contents of the vessel, but large enough to have an average value of intensive properties such as concentration and population density independent of random molecular variation. The age and the residual lifetime (or life expectancy; Zwietering, 1959) constitute the additional time-coordinate properties. An age, ψ, and a residual lifetime, ξ, for a point in the system are always related by

$$\psi + \xi = \theta \tag{22}$$

where θ is the dimensionless residence time for this particular point. Here ψ, ξ, and θ are assumed to be deterministic quantities. A point enters system with $\psi = 0$ and $\xi = \theta$, and leaves with $\psi = \theta$ and $\xi = 0$.

Completely segregated vessels may be imagined to have mixing between clumps with differing ages, but this mixing takes place at the vessel exit where the various clumps having $\xi = 0$ merge to form the outlet stream. The mixing occurs when $\psi = \theta$ for all clumps (but different clumps will have different values of $\psi = \theta$). Thus, whatever mixing there is between points with differing ages will occur as late as possible, namely, at the vessel outlet. Two kinds of mixing that can be allowed between points without altering the RTD for the system are possible. Mixing between points having the same age is always possible; but since these points have the same composition this is equivalent to no mixing at all and the system remains segregated. For mixing between points having different ages, Zwietering (1959) pointed out that such mixing is possible only when the points have the same residual lifetime. In the maximum mixedness case fresh feed enters the system with age $\psi = 0$ and immediately mixes with the material already in the vessel, which has many different ages but the same residual life. When mixing occurs between two groups with different ages, one of the groups will have $\psi = 0$. Thus mixing occurs as early as possible.

Table 6. CSD Dynamics and Control

Authors	Configuration (System)	Kinetics	Technique	Remarks
Miller and Saeman (1947)	Oslo (NH_4NO_3)		Experimental	Unstable and cyclic operation in classified crystallizer.
Saeman (1956) Saeman (1961)	MSMPR/MSCPR Vacuum (NH_4NO_3)	$G = k_g \Delta c$ B = seeding rate	Experiments with plant	Control of CSD by fines removal.
Randolph and Larson (1962)	Class II MSMPR [$(NH_4)_2SO_4$]	$G = k_g \Delta c_4$ $B = k_b \Delta c$	Solution to population balance and frequency response analysis	Transients of CSD; cycling due to fines dissolution.
Hulburt and Katz (1964)	Processing equipment	$G = G(\Delta c, L)$ $B = B(\Delta c, L)$	Classical statistical mechanical formulation	Transients in particle technology with growth, nucleation and weak agglomeration.
Randolph and Larson (1965)	MSMPR	$B = K_R G^i$	Analog simulation; frequency response; Routh Horwitz stability	Transients, stability, and its criteria.
Murray and Larson (1965)	MSMPR salting-out (ammonium alum-ethanol-water)	$B = K_R G^2$	Experimental and analog simulation	Verification of kinetics from transients
Sherwin et al. (1967)	MSMPR	$G = G(\Delta c) G(L)$ $G(\Delta c) = k_g \Delta c$ $G(L) = 1$ or $(1 + \alpha L)$ $B = B_{\mathrm{Volmer}}$ or B_{Mier}	Linear and nonlinear dynamics; Routh Horwitz stability	Cycling behavior; amplitude fluctuation by numerical nonlinear analysis.
Timm and Larson (1968)	MSMPR salting-out (alum-ethanol-H_2O) ($(NH_4)_2SO_4$-methanol-H_2O) (NaCl-ethanol-H_2O)	$B = K_R G^i$	Experimental and digital simulation	Verification of kinetics by transients.
Sherwin et al. (1969)	MSCPR	$G = k_g \Delta c$ $B = B_{\mathrm{Volmer}}$ or B_{Mier}	Linear and nonlinear dynamics; Nyquist stability	Cyclic behavior due to classification. Seeding and mixed product removal have stabilizing effect.
Hulburt and Stefango (1969)	MSMPR with fines removal	$G = k_g \Delta c$ $B = B_{\mathrm{Volmer}}$	Linearized moment equations	Negligible oscillations due to fines removal. Recycle magma has stabilizing effect.
Han (1969)	Class I MSMPR	$G = k_g \Delta c$ $B = B_{\mathrm{Volmer}}$	Analog simulation of linear and nonlinear dynamics	Self-induced oscillation; feedforward controller.
Mullin and Nyvlt (1970)	MSMPR/MSCPR ($Na_2S_2O_3 5H_2O$)	$G = 0.015\, \Delta c$ $B = (0.01 \sim 1.0)\, \Delta c^{3.8}$	Experimental and digital simulation on 200L pilot DTB unit	Periodic cyclic behavior.
Lei et al. (1971a,b)	MSMPR with fines trap	$G = k_g \Delta c$ $B = B_{\mathrm{Mier}}, K_R G^i$ B_{Volmer}	Linearized stability analysis by Routh Horwitz test; dynamics with nonlinear equations; numerical analysis	Stabilization effect of fines trap at large product size. Stable limit cycle around unstable equilibrium point. Feedback control system.
Gupta and Timm (1971)	Class II MSMPR	$B = K_R G^i$	Stability of feed-forward/backward control scheme; frequency response analysis	Control over fines may eliminate the sustained limit cycle. Bode diagram approximates first-order behavior.
Anshus and Ruckenstein (1973)	MSMPR	$G = G(\Delta c, L)$ $B = B(\Delta c, L)$	Linear stability analysis by Laplace transform, roots of characteristic equations	Stability criteria.
Randolph et al. (1973)	Class II MSCPR with fines removal (*R-z*)	$B = K_R G^i M_T^j$	Use of spectral technique to the linearized dynamics	Fines removal has stabilizing effect while classification has destabilizing effect.
Yu and Douglas (1975)	Class I MSMPR	$G = k_g \Delta c$ $B = B_{\mathrm{Volmer}}$	Linear stability by Routh Horwitz test; theory of nonlinear oscillation	Oscillatory operation may be advantageous because of high yield; evaluation of method of analysis.

(Table Continued)

Table 6. (Continued)

Authors	Configuration (System)	Kinetics	Technique	Remarks
Song and Douglas (1975)	Class I MSMPR ($NaCl$-ethanol-H_2O)	$G = 2.5\,\Delta c$ $B = 7 \times 10^4 \exp \left(\frac{-0.12}{(s-1)^2}\right)$	Experimental	Self-generated oscillations; sensitivity to kinetics.
Liss and Shinnar (1976)	MSMPR	$G = G(\Delta c, L)$ $B = B(\Delta c, \mu_i)$	Linear stability analysis by the Routh Horwitz test	Cycling phenomena due to magma dependent kinetics at low apparent values of sensitivity parameter.
de Leer et al. (1976)	Class II MSCPR with fines removal	$B = K_R G^i M_T^j$	Linear stability; roots of characterization equation.	Stability limits; nonlinear study desirable.
Shields (1976)	MSMPR evaporative, Two-stage cascade, Batch cooling	$G = k_g \exp (-E_G/R_g T)\,\Delta c^g$ $B = k_b\,\Delta c\,M_T^j$	Experimental and simulation of dynamics	Mode of operation and process configuration important on plant and lab studies.
Randolph et al. (1977)	Class II MSCPR with fines destruction loop (R-z) (KCl-H_2O)	$G = k_g\,\Delta c$ $B = 0.66 G^5\,M_T^{0.15}$	Experimental and numerical simulation of dynamics	Low-order cycling.
Randolph and Beckmann (1977)	Class II MSCPR with fines destruction loop (R-z)	$G = k_g\,\Delta c$ $B = K_R G^i\,M_T^j$	Simulation of dynamics and control by computer simulator	Efficient control policy of proportional control of nuclei density by manipulation of fines.
Aeschbach and Bourne (1979)	Continuous (hexamethylene tetramine)		Experimental	Dynamics and stability of weakly agitated crystallizer to its suspension characteristics.
Randolph (1980)	—	—	—	General review.
Ishii and Randolph (1980)	Class II MSMPR	$G = G^o G(L)$ where $G(L) = 1,\ L < L_1$ $= a,\ L > L_1$	Linearization and spectral density analysis	Stability limits.
Randolph and Rowang (1980)	MSMPR with fines trap (KCl)	$G = G(\Delta c)$ $B = K_R G^i$	Experimental on-line measurement of kinetics	Control of CSD.
Epstein and Sowul (1980)	Class II MSMPR	$G = k_g \Delta c$ $B = k_b \Delta c^b\,\mu_j$	Nonlinear stability by phase space analysis using computer simulation	Regions of system stability and occurrence of limit cycle by use of two-dimensional phase plane projectories and three-dimensional computer generated displays.
Randolph et al. (1981) and Randolph and Low (1982)	MSMPR with fines removal (KCl)	$B = K_R G^i$	Experimental	On-line CSD measurement technique; on-line control of CSD using proportional control of nuclei density by manipulation of fines.
Rousseau and Howell (1982)	MSCPR with fines removal (KCl)	$B = K_R G^i$	Experimental and simulation	Control scheme using Δc as variable and flow through fines trap as controlled variable.
Hashemi and Epstein (1982)	Nonisothermal continuous	Experimental kinetics	Multivariable system approach	Observability and controllability considerations.
Jerauld et al. (1983)	MSMPR	$G = k_g \Delta c$ $B = B_{\text{Volmer}}$	Linearized stability analysis; Hopf bifurcation	Conditions of limit cycle.
Akoglu et al. (1984)	MSMPR cooling (alum)	$G = k_g \exp (-E_G/R_g T)\Delta c^g$ $B = k_b \exp (-E_B/R_g T)\Delta c^b$	Linear dynamics includes energy balance	Transients; temperature effect.

Table 6. (Continued)

Authors	Configuration (System)	Kinetics	Technique	Remarks
Heiskanen and Norden (1984)	MSMPR with fines dissolution	$B = K_R G^i M_T^j$	Double Laplace transform of linearized dynamic equations	Dynamics and stability analysis.
Tavare and Garside (1985)	MSMPR	$G = k_g \Delta c^g$ $B = k_b \Delta c^b M_T^j$	Mass balance	Concentration multiplicity.
Tavare et al. (1985a)	MSMPR cooling	$G = k_g \exp(-E_G/R_g T)\, \Delta c^g$ $B = k_b \exp(-E_B/R_g T)\, \Delta c^b M_T^j$	Mass and energy balances	Temperature multiplicity.

Models for limits of micromixing

The two limits on mixing between points having different age can be represented by simple piston flow models as shown in Figure 8. Completely segregated crystallizers can be modeled as a single piston flow crystallizer with side exits as shown in Figure 8b, or as piston flow vessels in parallel as in Figure 8c. Some thought will show that these configurations are equivalent. The parallel vessels conform to the definition of complete segregation since each parallel element corresponds to the path followed by a point. The single plug flow vessel model has mixing in the radial direction and thus has mixing between points in violation of the intuitive definition of complete segregation. However, the mixing within the crystallizer occurs only between points having the same age and thus the same property attributes. Such mixing has no effect on performance characteristics, and the outlet conditions will be the same for these cases. The distribution of the side exits in a single plug flow vessel model or the length of parallel elements is arranged to duplicate the RTD for the system.

The element or the point in a completely segregated system can be considered as a small batch crystallizer. The population balance equation for such a clump with negligible attrition and agglomeration effects is

$$\frac{\partial \hat{n}}{\partial \psi} + G_T \frac{\partial \hat{n}}{\partial L} = 0 \tag{23}$$

where G is the size-independent overall linear growth rate. Here the total solvent capacity of the clump may be time-varying. It is therefore convenient to define the population density and the other specific quantities on the basis of total working solvent capacity of the clump; such quantities will be represented by $\wedge$ above the corresponding symbol.

The moment transformation of Eq. 23 with respect to size yields

$$\frac{d\hat{\mu}_0}{d\psi} = \hat{B}_T \tag{24}$$

$$\frac{d\hat{\mu}_1}{d\psi} = G_T \hat{\mu}_0 \tag{25}$$

$$\frac{d\hat{\mu}_2}{d\psi} = 2G_T \hat{\mu}_1 \tag{26}$$

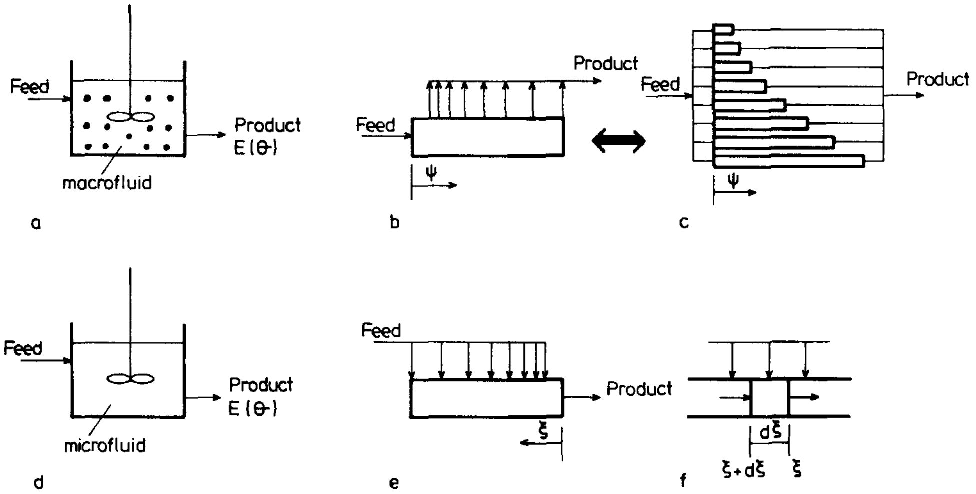

Figure 8. Extremes of micromixing.

a. Completely segregated vessel
b. Plug flow vessel with side exits
c. Plug flow elements in parallel
d. Maximum mixedness vessel
e. Plug flow vessel with side entrances
f. Differential element of configuration e

$$\frac{d\hat{\mu}_3}{d\psi} = 3G\tau\hat{\mu}_2 \tag{27}$$

with boundary conditions

$$\hat{\mu}_j = 0 \quad \text{at } \psi = 0 \quad j = 0, 1, 2, 3 \tag{28}$$

The variation of crystal size starting from $L = 0$ in the batch clump may be represented by

$$\frac{dL}{d\psi} = G\tau \tag{29}$$

The general supersaturation balance for a batch clump at any age ψ is

$$\frac{d\hat{\Delta c}}{d\psi} + \frac{d\hat{c}^*}{d\psi} + \frac{d\hat{W}}{d\psi} = 0 \tag{30}$$

and the solute balance is

$$\frac{d\hat{c}}{d\psi} + \frac{d\hat{W}}{d\psi} = 0 \tag{31}$$

The average population density of the product and the mean supersaturation and concentration of the crystallizing component at the vessel outlet are the expected average values of all the elements over the RTD, and are therefore given by

$$\bar{\hat{n}}(L) = \int_o^\infty \hat{n}(L, \psi)_{\text{batch}}\, E(\psi) d\psi \tag{32}$$

$$\overline{\hat{\Delta c}} = \int_o^\infty \hat{\Delta c}(\psi)_{\text{batch}}\, E(\psi) d\psi \tag{33}$$

$$\bar{\hat{c}} = \int_o^\infty \hat{c}(\psi)_{\text{batch}}\, E(\psi) d\psi \tag{34}$$

In order to facilitate easy evaluation of the integrals in Eqs. 33 and 34 they can be transformed into differential equations as

$$\frac{d\tilde{\tilde{\Delta c}}}{d\psi} = \hat{\Delta c}(\psi)_{\text{batch}}\, E(\psi) \tag{35}$$

and

$$\frac{d\tilde{\hat{c}}}{d\psi} = \hat{c}(\psi)_{\text{batch}}\, E(\psi) \tag{36}$$

with

$$\Delta\tilde{\hat{c}} = 0 \quad \text{and} \quad \tilde{\hat{c}} = 0 \quad \text{at } \psi = 0 \tag{37}$$

The values of $\tilde{\tilde{\Delta c}}$ and $\tilde{\hat{c}}$ determined by integration of Eqs. 35 and 36 for $\psi \rightarrow \infty$ will equal $\overline{\hat{\Delta c}}$ and $\bar{\hat{c}}$, respectively.

Simultaneous solutions of the set of differential equations (Eqs. 24–27, 29–31, 35–36) and partial differential equation 23 will define the completely segregated vessel.

In the maximum mixedness case fresh feed enters the system with age $\psi = 0$ and immediately mixes throughout the entire vessel cross section with points having many different ages but all having the same residual life, ξ. Figure 8e depicts a general model for the maximum mixedness configuration. The feed stream now enters the vessel through a variety of side entrances distributed along the vessel length to duplicate the arbitrary RTD. Although the situation is merely a reversal of the flow direction in Figure 8b, it represents an opposite extreme of mixing between the points with different ages, an extreme where mixing occurs at the vessel inlet and is thus as early as possible. The performance equations describing the system in a maximum mixedness case may be derived from the differential balances (Figure 8f) and follow similar lines to that of Zwietering (1959) in a chemical reactor case. The solute concentration balance is

$$-\frac{dc}{d\xi} = \Lambda(\xi)(c_i - c) - M_{Tmm} \tag{38}$$

and the corresponding supersaturation balance is

$$-\frac{d\Delta c}{d\xi} = \Lambda(\xi)(\Delta c_i - \Delta c) - M_{Tmm} + k_{mm} \tag{39}$$

where M_{Tmm} represents the dimensionless solid deposition rate and k_{mm} the dimensionless supersaturation generation rate. The appropriate boundary conditions associated with Eqs. 38 and 39 are that both $c(\xi)$ and $\Delta c(\xi)$ are bounded and positive for ξ. Usually it means that

$$\frac{dc}{d\xi} = 0, \quad \frac{d\Delta c}{d\xi} = 0 \text{ at } \xi \rightarrow \infty \tag{40}$$

The population balance equation for the crystallizing component can be derived as

$$\frac{\partial n}{\partial \xi} + G\tau\frac{\partial n}{\partial L} + \Lambda(\xi)(n - n_i) = 0 \tag{41}$$

Any configuration with an arbitrary RTD can in general be treated. However, for simplicity a classical MSMPR crystallizer having $\Lambda(\xi) = 1$ and clear feed with conventional supersaturation-dependent growth and nucleation kinetics for the crystallizing system is assumed. The pertinent moment equations obtained through the moment transformation of Eq. 41 with respect to size are

$$\frac{d\mu_0}{d\xi} = B\tau - \mu_0 \tag{42}$$

$$\frac{d\mu_1}{d\xi} = G\tau\mu_0 - \mu_1 \tag{43}$$

$$\frac{d\mu_2}{d\xi} = 2G\tau\mu_1 - \mu_2 \tag{44}$$

$$\frac{d\mu_3}{d\xi} = 3G\tau\mu_2 - \mu_3 \tag{45}$$

with boundary conditions

$$\frac{d\mu_j}{d\xi} = 0 \text{ as } \xi \to \infty \quad j = 0, 1, 2, 3 \tag{46}$$

The valid and required set of solutions describing the maximum mixedness MSMPR configuration is

$$c_i - c = M_{Tmm} \tag{47}$$

$$\Delta c_i - \Delta c = M_{Tmm} - k_{mm} \tag{48}$$

$$n = \frac{B}{G}\exp\left(-L/G\tau\right) \tag{49}$$

$$M_{Tmm} = 6k_{v'}\rho_c\, B\, G^3\, \tau^4 \tag{50}$$

Becker and Larson (1969) modeled these two extreme micromixing limits in an MSMPR crystallizer for the case of crystallization from presupersaturated feed solutions. In order to compare the performance of these two configurations they used the same inlet supersaturation levels in each case. The analytical solution of the population balance equation for the first-order relative nucleation kinetics (i.e., $i = 1$) showed substantial differences in product CSD obtainable in these two extreme levels of micromixing.

Tavare (1985b) analyzed an MSMPR crystallizer in which the supersaturation was generated by any one of the conventional modes, namely, cooling, evaporation, or dilution technique. Several modes of operation at the two extreme micromixing levels were illustrated with numerical examples, and the performance characteristics were also compared with those obtained in the corresponding macromixing limit, i.e., plug flow configuration. At higher rates the mean product size for plug flow configuration typically fell between those for the other extreme micromixing cases of an MSMPR crystallizer. Thus the level of micromixing is more important than the level of macromixing in determining system performance. If however all the clumps in the crystallizer were maintained at a constant level of Δc throughout their sojourn, the micromixing effects were unimportant for such an operation. As the crystallization processes invariably involve complex kinetic events, the extremes of micromixing will not necessarily meet the optimality constraints required to provide the bounds on the performance characteristics (see also Nauman and Buffham, 1983).

Degree of segregation

Danckwerts (1958) proposed the degree of segregation J_s as a measure for micromixing in a flow reactor. It may also be considered for the solution in a crystallizer and defined as the variance of ages between the points in the crystallizer divided by the variance of ages of all the points in the crystallizer. Thus

$$J_s = \frac{\operatorname{var}\psi_P}{\operatorname{var}\psi} = \frac{\frac{1}{V}\int_V (\psi_P - \bar{\psi})^2\, dV}{\int_0^\infty (\psi - \bar{\psi})^2 I(\psi)\, d\psi} \tag{51}$$

where

ψ = age of a molecule in the crystallizer

$\bar{\psi}$ = mean age of all molecules in the crystallizer = $\int_0^\infty \psi I(\psi)\, d\psi$

ψ_P = mean age of all molecules within a point in the crystallizer = $\int_0^\infty \psi I_P(\psi)\, d\psi$

$I(\psi)$ = age distribution in the crystallizer

$I_P(\psi)$ = age distribution within the point P in the crystallizer

The solvent capacity integral $\int_V$ represents the sum over all the points.

Zwietering (1959) showed that the total variance in ages ($\operatorname{var}\psi$) is the sum of the variance in ages between the points ($\operatorname{var}\psi_p$) and the variance in ages within a point (σ_P^2). Therefore

$$J_s = 1 - \frac{\sigma_P^2}{\operatorname{var}\psi} \tag{52}$$

In complete segregation, $\sigma_P^2 = 0$ for all points and $J_s = 1$. For a maximum mixedness MSMPR crystallizer $\operatorname{var}\psi_P = 0$ and $J_s = 0$. Thus $0 < J_s < 1$. Zwietering (1959) observed that $J_s = 1$ is possible with any RTD, but $J_s = 0$ is possible only with an exponential distribution since $\operatorname{var}\psi_P > 0$ for any distribution other than the exponential. Thus the real range for J_s is $(J_s)_{\min} < J_s < 1$ where $(J_s)_{\min}$ depends on $E(\theta)$.

In order to characterize the extent of micromixing based on solid-side information an additional analogous quantity, the degree of segregation based on CSD, may be defined as

$$J_c = 1 - \frac{CV_P^2}{CV^2} \tag{53}$$

where CV is the coefficient of variation based on crystal size distribution. For a maximum mixedness MSMPR crystallizer $CV_P = CV$ and $J_c = 0$. In complete segregation CV_P is normally not equal to zero when both nucleation and growth occur within the point. However, if monodispersed seed crystals are assumed to grow without any nucleation and growth dispersion phenomena, then under such a hypothetical condition $CV_P = 0$ and $J_c = 1$. Thus for real crystallizers the range for J_c may be less restrictive and perhaps the coefficient of variation is a less sensitive measure of CSD.

A micromixing condition lying between complete segregation and maximum mixedness is one of partial segregation. Evaluation of degrees of segregation for such incomplete micromixing is difficult, as a knowledge of distribution functions within the point over the entire space system is needed. Again the degree of segregation cannot uniquely determine the history regarding specific quantities such as concentration and population density in a crystallizer, as it is characterized by the ratio of variance (Eqs. 52 and 53). It is in general only an average parameter of the vessel and may provide a common basis for model discrimination.

Mixing space

A qualitative but conceptually useful representation of micromixing is shown by the mixing space diagram of Figure 9 (Nauman and Buffham, 1983). The abscissa, labeled *Macromixing*, measures the breadth of the RTD. A possible scale of measurement for this axis is the dimensionless variance. The ordinate, labeled *Micromixing*, is really a measure of how important micromixing effects can be. A possible scale for this axis is the difference between maximum and minimum degree of segregation. Micromixing effects are unimportant for plug flow configuration and may have maximum importance for MSMPR crystallizers. Although there is no theoretical assurance that the extremes of mixing will bound the performance, a real crystallizer may lie within the normal region of Figure 9 and perhaps may have performance characteristics bounded within those of the three special configurations representing the apexes of the normal region. However, it is important to note that the crystallization process generally involves consecutive and/or competitive kinetic events and therefore the optimum performance may not necessarily lie along the boundaries of the normal region of mixing plane. A possibility of interior optima exits and boundaries representing the extremes of micromixing perhaps may not be linear for a given crystallizer configuration.

In all the above analyses a tacit assumption is that the feeds to the system are mixed or become mixed immediately upon entering. In order to consider the special features of unpremixed feeds (Treleaven and Tobgy, 1971; Ritchie and Tobgy, 1978) Garside and Tavare (1984, 1985) imagined an MSMPR crystallizer with two feed streams each of which contains a single reactant species. These two species can react together homogeneously, and when the fluid phase becomes supersaturated with respect to product resulting from the liquid phase reaction, crystallization occurs. All the product in both solid and liquid phases together with unconverted material leaves the crystallizer through a single outlet. Inside the crystallizer a suspension element constituting a point will in general consist of unreacted reactant species together with product in both phases.

Clearly no reaction whatsoever will occur if all the points within the crystallizer contain only one reactant species, i.e., all the elements of two feed streams containing only one component remain segregated throughout their sojourn in the vessel. In this situation the age and residual lifetime distributions of the points are irrelevant from the point of view of reaction and subsequent precipitation. On the other hand, if both the species do exist at the same point by virtue of some mixing between the feed populations after entry, there will be reaction and subsequent precipitation and the rates of both these processes will depend on the point species concentration. The point species concentration will be determined partly by the previous mixing between the two reactant species, and partly by the extent to which molecules emanating from the same feed stream but with different ages have mixed together. In general it is therefore necessary to distinguish between species and age mixedness in order to characterize the unpremixed feeds crystallizer. On the basis of this distinction it is possible to conceive four extreme states of mixing in unpremixed feed streams crystallizers at the four corners of the plane representing an MSMPR unit, as shown in Figure 9.

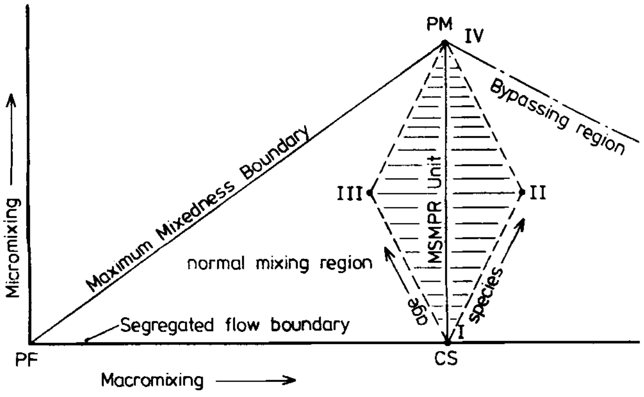

Figure 9. Schematic representation of mixing (Nauman and Buffham, 1983). PF, plug flow; CS, complete segregation; PM, perfect mixer.

I Complete species and age segregation
II Maximum species but minimum age mixedness
III Minimum species but maximum age mixedness
IV Maximum species and age mixedness

I. *Complete Species and Age Segregation.* If segregation between the species were complete, the two components would never mix and no reaction and subsequent crystallization would occur. Thus, no performance is a theoretical possibility whenever the reactant streams are unmixed, and it cannot be resolved simply from RTD measurement.

II. *Maximum Species but Minimum Age Mixedness.* In this situation points from each feed stream entering at the same time and having the same residual lifetime mix together immediately but do not mix with any other points having the same residual lifetime until the vessel exit. A total age segregation exists within the reactant populations.

III. *Minimum Species but Maximum Age Mixedness.* For completely immiscible feed streams it is likely that no mixing takes place between the feed streams although each stream is individually well-mixed. Again, the age and residual lifetime distributions of points are irrelevant from the point of view of reaction and subsequent precipitation.

IV. *Maximum Species and Age Mixedness.* All points of the same residual lifetime mix together as early as possible. This case refers to the maximum amount of mixing that can be achieved for a crystallizer having two feed streams.

Two limiting cases—maximum species but minimum age mixedness (case II) and maximum species and age mixedness (case IV)—were analyzed to explore the sensitivity of the two cases to the kinetic parameters used in chemical reaction and crystallization (Garside and Tavare, 1984, 1985). Under the condition of premixing of two reactants at the entry to the vessel, these two cases (II and IV) are tantamount to complete segregation and maximum mixedness, respectively, for a single-component reaction. All the results showed that although the differences between the conversions for a second-order reaction were small for the two extreme micromixing limits, significant influence on the product CSD was observed. In general the unpremixedness adds an additional dimension to the mixing space. The analysis was restricted to identical RTD functions of an MSMPR crystallizer for both the components. However the analysis with different, unequal RTD functions may be more complex and the performance characteristics may be different. For a case of mixing and reaction Treleaven and Togby (1971) pointed out that the unpremixed feeds to the reactor produced entirely different performance and may require an optimal micromixing policy in order to achieve optimum results.

Micromixing models

Process simulation studies (Garside and Tavare, 1984, 1985; Tavare, 1985b) have clearly demonstrated the enormous effect of the micromixing level on overall crystallizer performance. Although differences between the second-order reaction performances at the two extreme micromixing levels in all the cases of simulations (Garside and Tavare, 1984, 1985) are usually small, the significant influence on the product CSD may provide a comparatively sensitive and useful indicator of intermediate degrees of micromixing. The kinetic events for crystallization systems are generally nonlinear; crystallizers usually operate at relatively high yield; the RTD function is closer to that of an MSMPR unit; the physical nature of the crystallization process allows the practical possibility of segregation; and therefore micromixing effects may tend to be important in real crystallizers. Characterization of such micromixing effects in a real vessel at some intermediate micromixing level is of paramount importance for crystallization systems from both a theoretical and a practical viewpoint. As published work on the characterization of intermediate micromixing or partial segregation for crystallization configurations is scarce, the primary emphasis remains to examine critically the approaches used in the chemical reaction engineering literature and judge their suitability for crystallization systems. Although there is no general acceptance as to what constitutes a sufficient description of micromixing, a host of models describing specific mixing histories has been proposed for chemical reactors, each one of these models being an attempt to represent conceivable extreme or intermediate micromixing states with or without some mechanistic implications. Table 7 briefly outlines the major types of models that have appeared in the literature. The following section will discuss some aspects of micromixing models that may be of interest in crystallization research from a theoretical or predictive viewpoint. A detailed analysis will be avoided since only a few have been used in crystallization research.

Environment models

Formulation of models such as complete segregation and maximum mixedness for continuous crystallizers with any RTD function, depicted by plug flow vessels with side exits and entrances, respectively, represents the intrinsic micromixing level in an environment. If the solution in a crystallizer is considered to be a mixture of macrofluid with a fraction S and microfluid with the remaining fraction $(1 - S)$, the micromixedness ratio $[(1 - S)/S]$ should be a simple empirical measure of segregation state. The value of S may be determined by either reactive or nonreactive tracer systems (Villermaux and David, 1983). A similar measure from the solid-side information, the dimensionless segregation level for CSD, may be defined as

$$S_c = \frac{\bar{L} - \bar{L}_{mm}}{\bar{L}_{cs} - \bar{L}_{mm}} \tag{54}$$

Table 7. Micromixing Models

Environment Models	
Complete segregation	Danckwerts (1958)
Maximum mixedness	Zwietering (1959)
Segregation level (one-parameter)	Zoulalian and Villermaux (1974) Troung and Methot (1976) Hanley and Mischke (1978) Villermaux and David (1983)
Two-environment (one-parameter) Series or parallel	Ng and Rippin (1965) Weinstein and Alder (1967) Rippin (1967a) Villermaux and Zoulalian (1969) Nishimura and Matsubura (1970) Methot and Roy (1971) Rao and Edwards (1973) Goto and Matsubara (1975) Takao and Murakami (1976)
Reverse	Chen and Fan (1971) Tsai et al. (1971)
Environment Models (Continued)	
Spatial	Miyawaki et al. (1975) Apostolopoulos and Smith (1976)
Three-environment (two-parameter)	Ritchie and Togby (1979) Valderrama and Gordon (1979, 1981) Chai and Valderrama (1982)
Four-environment (three-parameter)	Mehta and Tarbell (1983)
Structured fluid flow network (multiparameter)	Asbjornsen (1965)
Recycle Models	
Recycle plug flow reactor	Gillespie and Carberry (1966) Fan et al. (1971)
Generalized recycle reactor	Szabo and Nauman (1969) Rippin (1967b) Dohan and Weinstein (1973) Dudukovic (1977a,b)
Coalescence and Redispersion Models (CRM)	
	Shain (1961) Curl (1963) Spielman and Levenspiel (1965) Kattan and Alder (1967, 1972) Harris and Srivastava (1968) Evangelista et al. (1969) Komasawa et al. (1969, 1971) Rao and Dunn (1970) Treleaven and Togby (1972) Zeitlin and Tavlarides (1972) Patterson (1975) Goto et al. (1975) Goto and Matsbura (1975) Villermaux (1981) Hsia and Tavlarides (1983) Marconi and Vatistas (1983)
IEM (Interaction by Exchange with the Mean) Models	
	Harada et al. (1962) Costa and Trivossi (1972a,b) Aubry and Villermaux (1975) David and Villermaux (1975) Plasari et al. (1978) Klein et al. (1980) Villermaux (1981) Pohorecki and Baldyga (1983a,b,c) Villermaux and David (1983)
Diffusion Models	
Packet diffusion	Rice et al. (1964) Mao and Toor (1970) Rao and Edwards (1971) Troung and Methot (1976) Nauman (1975) Nabholz et al. (1977) Belvi et al. (1981) Jenson (1983)
Deformed packet diffusion	Angst et al. (1982a,b) Bourne and Rohani (1983) Bolzern and Bourne (1983) Baldyga and Bourne (1984a)
Lamellar mixing	Ottino et al. (1979) Ranz (1979) Ottino (1980) Ou and Ranz (1983a,b, 1984) Ou et al. (1983) Ottino and Chella (1983, 1984)
Isotropic turbulent mixing	Pohorecki and Baldyga (1983a,b,c) Baldyga and Bourne (1984b,c,d)

where $\bar{L}$ is the product mean size. It is important to note that $\bar{L}_{mm}$ and $\bar{L}_{cs}$ may not necessarily be extreme bounds on the mean sizes.

Environment models for chemical reactors assume that the vessel volume consists of two or more separate environments having extreme states of micromixing. The reactor may be modeled either by splitting the feed into completely segregated and maximum mixedness environments and combining them at the reactor exit with no interaction among the parallel environments, or by sending the entire feed stream into a completely segregated entering environment and subsequently transferring it to a maximum mixedness leaving environment at a prescribed rate, the effluents of these series environments being combined at the vessel exit. Several other variations of environment models have been proposed that differ either in structure of environment interactions or in terms of transfer rates; see Table 7. Environment models are essentially system-specific and empirical in nature. Recently some mechanistic implications have been pointed out by establishing the analogy with the theory of isotropic turbulent mixing and its equivalence with other micromixing models (Ritchie, 1980; Mehta and Tarbell, 1983). However, these environment models have not been compared extensively against experimental results. They offer substantial computational economy and are relatively simple and easy to use.

Recycle models

A plug flow reactor with recycle can be used as a model of a flow reactor, with recycle ratio as a model parameter representing incomplete macromixing. When the recycle ratio tends to approach zero or infinity, the RTD of the plug flow recycle reactor approaches that of plug flow or that of CSTR, respectively. The recycle model in this case always implies that the system will be at maximum mixedness (Rippin, 1967b). The achievement of maximum mixedness is assumed to occur at the point where the recycle stream is mixed with fresh feed. The plug flow reactor (with $R = 0$ and $J_s = 1$) is simultaneously under the state of complete segregation and maximum mixedness, and the CSTR (with $R \rightarrow \infty$ and $J_s \rightarrow 0$) is always at the state of maximum mixedness.

A recycle reactor is not at maximum mixedness except when the vessel has a RTD function corresponding to one or more piston flow elements in parallel. For other RTD's the recycle reactor will have an intrinsic but intermediate level of micromixing. The generalized recycle reactor provides a two-parameter deterministic model that may describe the intermediate levels of micromixing for a given macromixing level. Tavare et al. (1985b) modeled a configuration of an MSMPR crystallizer cascade with magma recycle in order to use it as a micromixing model. In addition to the recycle model, other mutliparameter flow models may also be considered as micromixing models.

Coalescence and redispersion models

In coalescence and redispersion models (CRM) as originated by Curl (1963), micromixing in two-phase and/or miscible-fluid systems is viewed as a stochastic process in which the reactor volume is treated as an ensemble of fluid clumps which coalesce randomly, two at a time, at some characteristic frequency that is the mixing parameter of the model. The coalescence is followed by instantaneous homogenization of property-like concentration and redispersion into separate clumps of the same composition. Between interactions each clump is assumed to behave as a batch vessel. The various available models differ in the method of controlling the rate of mixing by coalescence and redispersion and in locating the fluid elements within either a spatial frame of reference or within a black box in which the location of a clump is defined by coordinates determined by RTD. The model parameter may be determined experimentally from either fast reaction mixing limited data or measurement of tracer fluctuations. One of the positive features of CRM is its analogy with the theory of isotropic turbulence in order to characterize the model parameter. The rigorous model description represented by an integro-partial differential equation is difficult to solve. Approximate analytical and numerical methods have been suggested with a limited applicability. Monte Carlo simulation techniques have also been used.

IEM (Interaction by Exchange with the Mean) models

In this type of model a typical clump is followed from its birth at the feed inlet. The clump is assumed to act as a batch vessel having uniform internal concentration and exchanging matter with an environment whose concentration is taken to be the mean concentration at any time of all the clumps in the vessel. The average concentration of the vessel contents is determined by summing the product of the age $I(\psi)$ and concentration in the clump at any time over all clumps (similar to Eq. 34). The concentration in a clump is not determined uniquely by the reaction kinetics and macromixing, but also by the micromixing; therefore solution of the model equations requires an iterative procedure. The model assumes that micromixing is characterized by a single parameter termed the micromixing time constant. If the micromixing time constant approaches zero the microfluid and the maximum mixedness limit is reached, while for infinity the system is completely segregated and in a state of macrofluid. The model parameter, the micromixing time constant, can either be determined experimentally or predicted from the theory of isotropic turbulence and is comparable to that of CRM. However when the degree of segregation is high and the concept of average concentration becomes less than realistic, the predictions of the model differ considerably from those of CRM. The process of turbulent erosion, where large clumps are gradually peeled off and shrink in losing matter to produce a well-mixed microfluid, can be modeled by the IEM model with different process time constants (Villermaux and David, 1983).

Diffusion models

IEM models use a concept of external resistance to the segregated element, and convective fluxes make the predominant contribution to mass transfer. The model description uses ordinary differential equations containing a single model parameter. In the category of packet diffusion models the clumps have an internal concentration gradient and mass transfer within the segregated clump is considered to be the controlling mechanism. Diffusive mass transfer is more significant than convection because of small clump size. The shape of an element is usually a well-defined geometry like a slab, cylinder, or sphere, and the unsteady-state, one-dimensional diffusion equation without the convective term but incorporating the reaction has been considered with two boundary conditions. In all these cases the shape and size of the element have remained unchanged during diffusion and reaction, the model parameter being the size of element. The packet diffusion models are versatile in that they can treat any reaction scheme for a given reactor configuration and can be used as an adjustable empirical model. The model parameter representing the size of the element may be predicted from the theory of isotropic turbulence. Recently, deformed packet diffusion models have been used to account for the laminar deformation of the reaction zone by shear or extensional flow.

In lamellar mixing models the similarity in reactive mixing between laminar and turbulent regions in small elementary volumes in a Lagrangian frame is used. In this approach the flow is modeled as a population of microflow elements in each of which the instantaneous flow is homogeneous. Such elements exhibit a lamellar structure whose component striations exchange matter by molecular diffusion and reduce the thickness with time as a consequence of uniform fluid deformation enhancing the diffusion process. Over the microflow element the unsteady state diffusion equation with reaction and convection terms is used. Averages are introduced only late in the analysis, thus allowing considerable flexibility in adjusting the degree of sophistication of the mathematical description of the underlying process. Lamellar mixing models provide an alternative approach to modeling the complex interactions between local motion, molecular diffusion, and chemical reaction in the mixing of miscible reactive fluids.

Pohorecki and Baldyga (1983a, b) proposed using the spectral interpretation of mixing in an isotropic turbulent field in order to explain micromixing effects in homogeneous liquid phase chemical reactors. The authors in their further work (1983c) used the same model to evaluate the influence of the intensity of mixing on the rate of precipitation in an agitated, perfectly macromixed vessel. Baldyga and Bourne (1984b, c, d) presented a micromixing model based on information from fluid mechanics. The concentration spectrum indicates that molecular diffusion starts toward the fine-scale end of the viscous-convective subrange and becomes dominant in the viscous-diffusive subrange. Such small fluid elements are subject to laminar deformation, and the one-dimensional diffusion equation is then valid. The role of vorticity for small eddies in providing the mechanism to form a laminar structure by engulfing the fluid in their environment is important. Diffusion and reaction occur within a deforming laminated structure temporarily trapped inside the stretching vortices. Mixing brought about by these periodic processes ends when the concentration is uniform at the molecular scale.

Concluding Remarks

This paper constitutes a review of some of the important work, mainly over the past three decades, on mixing and related areas in continuous crystallizers. This accumulated effort has now firmly established a formalized unifying approach of chemical reaction engineering to the analysis of crystallization processes. A comprehensive treatment of macro- and micromixing applied to crystallization configuration has been presented with due emphasis on the modeling efforts.

The approach considered here lays no claim to providing a detailed physical insight into the interaction of mixing and crystallization, but provides rather a means of evaluating and subsequently predicting performance for given crystallizer configurations. The basis of the general technique is the use of a known crystallization system to evaluate the parameters of a model that represents by simulation the performance obtained experimentally from the crystallizer. To this more limited end the success of any model must lie in its possessing mixing parameters that are a function of the hydrodynamic conditions in the crystallizer alone and that exhibit no correlation with crystallization kinetic parameters. A complete set of experimental data and a powerful parameter characterization technique would be necessary to determine the model parameters and subsequently relate them to crystallizer hydrodynamics.

Significant progress has been achieved with regard to the problem of crystal size distribution and its many interactions with design, analysis, and operation of crystallizers, but gaps in our understanding still exist, particularly in the area of micromixing. Results to date suggest that there is a need for simultaneous development in several areas, such as efficient algorithms for model evaluation, reliable means for model characterization, clever experimental designs for model verification, and simple but powerful techniques for model discrimination. Such attempts will certainly be useful in increasing our understanding of mixing in continuous crystallizers.

Notation

A_T = total crystal surface area, m^2/kg solvent
b = nucleation order
B = nucleation rate, number/s · kg solvent
c = concentration, kg/kg
c^* = saturation concentration, kg/kg
Δc = concentration driving force, kg/kg
CV = coefficient of variation based on CSD
$E(\theta)$ = dimensionless residence time distribution function, dimensionless exit age distribution
E_B = activation energy for nucleation, kJ/mol
E_G = activation energy for growth, kJ/mol
$F(\theta)$ = dimensionless cumulative residence time distribution younger than θ
g = growth rate order, dimensionless growth rate function
G = linear growth rate, m/s
$H(\theta)$ = response of the system as a function of dimensionless age (or time)
i = relative kinetic order ($= b/g$)
$I(\theta)$ = dimensionless internal age distribution
j = index variable, exponent of magma density in nucleation correlation
J = degree of segregation
k = dimensionless supersaturation generation rate, stage number
k_a = area shape factor
k_b = nucleation rate coefficient, number/[s · kg(kg/kg)^b(kg/kg)^j]
k_g = growth rate coefficient, m/[s(kg/kg)^g]
k_v = volume shape factor
K_R = relative nucleation rate coefficient, no/(s · kg(m/s)^i(kg/kg)^j}
L = crystal size, m
m = parameter in breakage model
M = solid concentration, kg/kg
$M(L)$ = solid concentration between L and $L + dL$, kg/kg
M_T = magma density, kg/kg; dimensionless solid deposition rate
n = population density, number/kg · m
n^0 = nuclei population density, number/kg · m
p = Laplace transform variable with respect to dimensionless time
$Q(\theta)$ = arbitrary input function
R = dimensionless parameter in R-z crystallizer model equal to ratio of withdrawal of fines at size L to MSMPR rate
R_g = universal gas constant, kJ/mol · K
s = supersaturation ratio ($= c/c^*$)

S = fractional capacity of macrofluid, segregation level
t = time, age, s
T = absolute temperature, K
V = solvent capacity, kg
var = variance
x = dimensionless crystal size ($=L/G\tau$)
y = dimensionless population density ($=n/n^o$)
W = crystal mass, kg/kg
z = dimensionless parameter in R-z crystallizer model equal to ratio of withdrawal of product at size L to MSMPR rate

Greek letters

α, β = model parameters in size-dependent growth rate models
$\alpha_1, \beta_1, \beta_2$ = model parameters in classification functions
β_3 = breakage model parameter
$\gamma = \sqrt{1 + (4/Pe)}$
Λ = dimensionless residence time and crystal size intensity function
θ = dimensionless residence time ($=t/\tau$); dummy variable
λ = dimensionless classification function
μ_j = jth moment of size distribution, number $\cdot$ m^j/kg
ξ = dimensionless residual lifetime
ϕ = mass fraction of the distribution around the mean
ψ = dimensionless age
ρ = dimensionless growth rate
ρ_c = crystal density, kg/m^3
σ^2 = variance
τ = mean residence time, s

Subscripts

batch = value evaluated for batch case
c = crystallizer, crystal
cs = complete segregation
C = threshold for classification
$F, F1$ = threshold for fines removal
i = inlet, initial
mm = maximum mixedness
p = product
P = point, clump
s = solution
w = weight distribution

Superscripts

$\dot{}$ = derivative with respect to θ
$\bar{}$ = mean or transformed quantity
$\hat{}$ = quantity based on total solvent capacity of the crystallizer
$\tilde{}$ = dummy variables

Literature Cited

Abegg, C. F., and N. S. Balkrishnan, "The Tanks-in-Series Concept as a Model for Imperfectly Mixed Crystallizers," *Chem. Eng. Prog. Symp. Ser.* No. 110, **67**, 88 (1971).

Abegg, C. F., J. D. Stevens, and M. A. Larson, "Crystal Size Distributions in Continuous Crystallizers when Growth Rate is Size-Dependent," *AIChE J.*, **14**, 118 (1968).

Aeshbach, S., and J. R. Bourne, "The Attainment of Homogeneous Suspension in a Continuous Stirred Tank," *Chem. Eng. J.*, **4**, 234 (1972).

———, "Influence of the Degree of Crystal Suspension on Crystallizer Stability," in *Industrial Crystallization 1978*, S. J. Jancic and E. J. de Jong, Eds., North Holland, Amsterdam, 259 (1979).

Akoglu, K., N. S. Tavare, and J. Garside, "Dynamic Simulation of a Nonisothermal MSMPR Crystallizer," *Chem. Eng. Commun.*, **29**, 353 (1984).

Angst, W., J. R. Bourne, and R. N. Sharma, "Mixing and Fast Chemical Reaction. IV: The Dimensions of the Reaction Zone," *Chem. Eng. Sci.*, **37**, 585 (1982a).

———, "Mixing and Fast Chemical Reaction. V: Influence of Diffusion within Reaction Zone on Selectivity," *Chem. Eng. Sci.*, **37**, 1,259 (1982b).

Anshus, B. E., and E. Ruckenstein, "On the Stability of a Well-Stirred Isothermal Crystallizer," *Chem. Eng. Sci.*, **28**, 501 (1973).

Apostolopoulos, G. P., and W. D. Smith, Jr., "A New Model for Micromixing in Chemical Reactors," ISCRE4, Heidelberg (Apr., 1976).

Asbjornsen, O. A., "Incomplete Mixing Simulated by Fluid Flow Network," *AIChE–ICE Symp. Ser.*, **10**, 40 (1965).

Aubry, C., and J. Villermaux, "Representation du mélange impartfait de deux courants de reactifs dan du récteur agité continu," *Chem. Eng. Sci.*, **30**, 457 (1975).

Baldyga, J., and J. R. Bourne, "Mixing and Fast Chemical Reaction. VIII: Initial Deformation of Material Elements in Isotropic Homogeneous Turbulence," *Chem. Eng. Sci.*, **39**(2), 329 (1984a).

———, "A Fluid Mechanical Approach to Turbulent Mixing and Chemical Reaction. I: Inadequacies of Available Models," *Chem. Eng. Commun.*, **28**, 231 (1984b).

———, "A Fluid Mechanical Approach to Turbulent Mixing and Chemical Reaction. II: Micromixing in the Light of Turbulence Theory," *Chem. Eng. Commun.*, **28**, 243 (1984c).

———, "A Fluid Mechanical Approach to Turbulent Mixing and Chemical Reaction. III: Computational and Experimental Results for the New Micromixing Model," *Chem. Eng. Commun.*, **28**, 259 (1984d).

Becker, G. W., Jr., and M. A. Larson, "Mixing Effects in Continuous Crystallization," *Chem. Eng. Prog. Symp. Ser.* No. 95, **65**, 14 (1969).

Belvi, H., J. R. Bourne, and P. Rys, "Mixing and Fast Chemical Reaction. III: Diffusion-Reaction Model for the CSTR," *Chem. Eng. Sci.*, **36**(10), 1649 (1981).

Bennett, R. C., "Product Size Distribution in Commercial Crystallizers," *Chem. Eng. Prog.*, **58**(9), 76 (1962).

Berglund, K. A., and M. A. Larson, "Modeling of Growth Rate Dispersion of Citric Acid Monohydrate in Continuous Crystallizers," *AIChE J.*, **30**(2), 280 (1984).

Bolzern, O., and J. R. Bourne, "Mixing and Fast Chemical Reaction. VI: Extension of the Reaction Zone," *Chem. Eng. Sci.*, **38**(7), 999 (1983).

Bourne, J. R., "Hydrodynamics of Crystallizers with Special Reference to Classification," in *Industrial Crystallization 1978*, S. J. Jancic and E. J. de Jong, Eds., North Holland, Amsterdam, 215 (1979).

Bourne, J. R., and S. Rohani, "Mixing and Fast Chemical Reaction. VII: Deforming Reaction Zone Model for the CSTR," *Chem. Eng. Sci.*, **38**(6), 911 (1983).

Bourne, J. R., and M. Zableka, "The Influence of Gradual Classification on Continuous Crystallization," *Chem. Eng. Sci.*, **35**, 533 (1980).

Bransom, S. H., "Factors in the Design of Continuous Crystallizers," *Brit. Chem. Eng.*, **5**, 838 (1960).

———, "Continuous Crystallizer Design," *Chem. Proc. Eng.*, **46**(12), 647 (1965).

Broadfoot, R., and E. T. White, "Performance Charts for Continuous Pans," *Proc. Qld. Soc. Sugar Cane Tech.* (1975).

Canning, T. F. and A. D. Randolph, "Some Aspects of Crystallization Theory: Systems that Violate McCabe's ΔL Law," *AIChE J.*, **13**, 5 (1967).

Chai, C., and J. O. Valderrama, "A New Approach to View Partial Segregation Models in Chemical Reactors," *Chem. Eng. Sci.*, **37**(3), 494 (1982).

Chapman, C. M., et al., "Particle-Gas-Liquid Mixing in Stirred Vessels. I: Particle-Liquid Mixing," *Chem. Eng. Res. Des.*, **61**, 71 (1983).

Chen, M. S. K., and L. T. Fan, "A Reversed Two-environment Model for Micromixing in a Continuous Flow Reactor," *Can. J. Chem. Eng.*, **49**, 704 (1971).

Costa, P., and C. Trevissoi, "Some Kinetic and Thermodynamic Features of Reactions between Partially Segregated Fluids," *Chem. Eng. Sci.*, **27**, 653 (1972a).

———, "Reactions with Nonlinear Kinetics in Partially Segregated Fluids," *Chem. Eng. Sci.*, **27**, 2,041 (1972b).

Curl, R. L., "Dispersed-phase Mixing. I: Theory and Effects in Simple Reactors," *AIChE J.*, **9**, 175 (1963).

Danckwerts, P. V. "Continuous-flow Systems: Distribution of Residence Times," *Chem. Eng. Sci.* **2**, 1 (1953).

———, "The Effect of Incomplete Mixing on Homogeneous Reactions," *Chem. Eng. Sci.* **8**, 93 (1958).

David, R., and J. Villermaux, "Micromixing Effects on Complex Reactions in a CSTR," *Chem. Eng. Sci.*, **30**, 1,309 (1975).

de Leer, B. G. M., A. Koning, and E. J. de Jong, "Stability and Dynamic Behavior of Crystallizers," in *Industrial Crystallization*, J. W. Mullin, Ed., Plenum Press, New York, 391 (1976).

Dohan, L. A., and H. Weinstein, "Generalized Recycle Reactor Model for Micromixing," *Ind. Eng. Chem. Fundam.*, **12**(1), 64 (1973).

Dudukovic, M. P., "Micromixing Effects on Multiple Steady States in Isothermal Chemical Reactors," *Chem. Eng. Sci.*, **32**, 985 (1977a).

———, "On the Use of the Generalized Recycle Model to Interpret Micromixing in Chemical Reactors," *Ind. Eng. Chem. Fundam.*, **16**, 385 (1977b).

Epstein, M. A. F., and L. Sowul, "Phase Space Analysis of Limit Cycle Development in CMSMPR Crystallizers Using Three-dimensional Computer Graphics," *AIChE Symp. Ser.* No. 193, **76**, 6 (1980).

Evangelista, J. J., S. Katz, and R. Shinnar, "Scale-up Criteria for Stirred Tank Reactors," *AIChE J.*, **15**, 843 (1969).

Fan, L. T., B. I. Tsai, and L. E. Erickson, "Simultaneous Effects of Macromixing and Micromixing on Growth Processes," *AIChE J.*, **17**(3), 689 (1971).

Fitzgerald, T. J., and T. Yang, "Size Distribution for Crystallization with Continuous Growth and Breakage," *Ind. Eng. Chem. Fundam.*, **11**(4), 588 (1972).

Garside, J., S. N. Das, and J. W. Mullin, "Growth and Dissolution Kinetics of Potassium Sulfate," *Ind. Eng. Chem. Fundam.*, **13**(4), 299 (1974).

Garside, J., and S. J. Jancic, "Prediction and Measurement of Crystal Size Distributions for Size-dependent Growth," *Chem. Eng. Sci.* **33**, 1,623 (1978).

Garside, J., V. R. Phillips, and M. B. Shah, "On Size-dependent Crystal Growth," *Ind. Eng. Chem. Fundam.*, **15**(3), 230 (1976).

Garside, J., and N. S. Tavare, "Mixing, Reaction, and Precipitation in an MSMPR Crystallizer: Effects of Reaction Kinetics on the Limits of Micromixing," in *Industrial Crystallization 84*, S. J. Jancic and E. J. de Jong, Eds., Elsevier, Amsterdam, 131 (1984).

———, "Mixing, Reaction, and Precipitation: Limits of Micromixing in an MSMPR Crystallizer," *Chem. Eng. Sci.*, **40**(8), 1,485 (1985).

Garside, J., et al., "The Relation between Growth Rate Dispersion and Mechanical Properties of Crystals," in *Industrial Crystallization 84*, S. J. Jancic and E. J. de Jong, Eds., Elsevier, Amsterdam, 459 (1984).

Gillespie, B. B., and J. J. Carberry, "Reactor Yield at Intermediate Mixing Levels—An Extension of Van de Vuss's Analysis," *Chem. Eng. Sci.*, **21**, 472 (1966).

Goto, H., S. Goto, and M. A. Matsubara, "A Generalized Two-environment Model for Micromixing in a Continuous Flow Reactor. II: Identification of Model," *Chem. Eng. Sci.*, **30**, 71 (1975).

Goto, S., and M. A. Matsubara, "A Generalized Two-Environment Model for Micromixing in a Continuous Flow Reactor. I: Construction of Model," *Chem. Eng. Sci.*, **30**, 61 (1975).

Grabenbauer, G. C., and C. E. Glatz, "Protein Precipitation—Analysis of Particle Size Distribution and Kinetics," *Chem. Eng. Commun.*, **12**, 203 (1981).

Groenweg, P., and T. Hoffman, "Modeling the Seeded Batch Crystallization of Alumina Trihydrate: A Method for Solving the Population Balance Equation," *Proc. 2nd World Cong., Chem. Eng.* **IV**, Montreal, 39 (1981).

Grootscholten, P. A. M., "Solid-Liquid Contacting Industrial Crystallizers and Its Influence on Product Size Distribution," Ph.D. Thesis, WTHD150, Laboratory for Process Equipment, Delft (Aug., 1982).

Grootscholten, P. A. M., et al., "Effect of Crystallizer Geometry on Crystallizer Performance," in *Industrial Crystallization 81*, S. J. Jancic, and E. J. de Jong, Eds., North Holland, Amsterdam, 189 (1982).

Grootscholten, P. A. M., E. J. de Jong, and A. Scrutton, "Chemical Engineering Approach to Industrial Crystallization," *Proc. 2nd World Cong., Chem. Eng.*, **IV**, Montreal, 59 (1981).

Grootscholten, P. A. M., A. Scrutton, and E. J. de Jong, "Influence of Crystal Breakage on Kinetics of Sodium Chloride Crystallization," *Chem. Eng. Res. Des.*, **63**(1), 34 (1985).

Gupta, G., and D. C. Timm, "Predictive-Corrective Control for Continuous Crystallization," *Chem. Eng. Prog. Symp. Ser.* No. 110, **67**, 116 (1971).

Halfon, A., and S. Kaliaguine, "Alumina Trihydrate Crystallization. 2: A Model of Agglomeration," *Can. J. Chem. Eng.*, **54**, 168 (1976).

Han, C. D., "A Control Study on Isothermal Mixed Crystallizers," *Ind. Eng. Chem. Process Des. Dev.*, **8**(2), 150 (1969).

Han, C. D., and R. Shinnar, "The Steady State Behavior of Crystallizers with Classified Product Removal," *AIChE J.*, **14**, 612 (1968).

Hanley, T. R., and R. A. Mischike, "A Mixing Model for a Continuous Flow Stirred Tank Reactor," *Ind. Eng. Chem. Fundam.*, **16**, 385 (1978).

Harada, M., et al., "Micromixing in a Continuous Flow Reactor (Coalescence and Redispersion Model)," *Memoirs Faculty of Eng.*, Kyoto Univ., **24**, 431 (1962).

Harris, I. J., and R. D. Srivastava, "The Simulation of Single-Phase Turbulent Reactors with Incomplete Reactant Mixing," *Can. J. Chem. Eng.*, **46**, 66 (1968).

Hashemi, R., and M. A. F. Epstein, "Observability and Controllability Considerations in Crystallization Process Design," *AIChE Symp. Ser.* No. 215, **78**, 81 (1982).

Heiskanen, T., and H. V. Norden, "Dynamics and Stability of an MSMPR Crystallizer with Fines Dissolving," *Acta Polytechnica Scandinavica, Chem. Tech. and Metallurgy Ser.* No. 158, Helsinki, 45 (1984).

Hill, S., "Residence Time Distribution in Continuous Crystallizers," *J. Appl. Chem.*, **20**, 300 (1970).

Hoare, M., "Protein Precipitation and Precipitate Aging. I: Salting-out and Aging of Casein Precipitates" *Trans. ICE*, **60**(2), 79 (1982a).

———, "Protein Precipitation and Precipitate Aging. II: Growth of Protein Precipitates During Hindered Settling or Exposure to Shear," *Trans. ICE*, **60**(3), 157 (1982b).

Holldroff, H., H. H. Emons, and H. Voigt, "Agglomeration Behavior of Potassium Chloride in the Process of Cooling Crystallization," Vortrag CHISA Conf., Usti nad Labem, Czechoslovakia (1975).

Hsia, M. A., and L. L. Tavlarides, "Simulation Analysis of Drop Breakage, Coalescence, and Micromixing in Liquid-Liquid Stirred Tanks," *Chem. Eng. J.*, **26**, 189 (1983).

Hulburt, H. M., and S. Katz, "Some Problems in Particle Technology: A Statistical Mechanical Formulation," *Chem. Eng. Sci.*, **19**, 555 (1964).

Hulburt, H. M., and D. G. Stefango, "Design Models for Continuous Crystallizers with Double Drawoff," *Chem. Eng. Symp. Ser.* No. 95, **65**, 50 (1969).

Ishii, T., and A. D. Randolph, "Stability of the High-yield MSMPR Crystallizer with Size-dependent Growth Rate," *AIChE J.*, **26**(3), 507 (1980).

Janse, A. H., and E. J. de Jong, "The Occurrence of Growth Dispersion and Its Consequences," in *Industrial Crystallization*, J. W. Mullin, Ed., Plenum, New York, 145 (1976).

Jenson, V. G., "A Model for Mixing with Fast Chemical Reactions," *Chem. Eng. Sci.*, **38**(8), 1,151 (1983);

Jerauld, G. R., Y. Vasatis, and M. F. Doherty, "Simple Conditions for the Appearance of Sustained Oscillations in Continuous Crystallizers," *Chem. Eng. Sci.*, **38**(10), 1,675 (1983).

Juzaszek, P., and M. A. Larson, "Influence of Fines Dissolving on Crystal Size Distribution in an MSMPR Crystallizer," *AIChE J.*, **23**(4), 460 (1977).

Kattan, A., and R. J. Alder, "A Stochastic Model for Homogeneous Turbulent Tubular Reactors," *AIChE J.*, **13**, 580 (1967).

———, "A Conceptual Framework for Mixing in Continuous Chemical Reactors," *Chem. Eng. Sci.*, **27**, 1,013 (1972).

Kau, T. B., and N. S. Torocheshikov, "Theory of Crystal Aggregation in Bulk Crystallization from Solution," *Theoretical Found. Chem. Eng.*, **16**, 222 (1982).

Kawashima, Y., Y. Kurachi, and H. Takenaka, "Preparation of Spherical Wax Matrices of Sulfamethoxazole by Wet Spherical Agglomeration Technique Using a CMSMPR Agglomerator," *Powder Technol.*, **32**, 155 (1982).

Kawashima, Y., M. Okumura, and H. Takenaka, "The Effects of Temperature on the Spherical Crystallization of Salicylic Acid," *Powder Technol.*, **39**, 41 (1984).

Klein, J. P., R. David, and J. Villermaux, "Interpretation of Experimental Liquid-Phase Micromixing Phenomena in a Continuous Stirred Reactor with Short Residence Times," *Ind. Eng. Chem. Fundam.*, **19**, 373 (1980).

Komasawa, I., T. Sasakura, and T. Otaka, "Behavior of Reacting and Coalescing Dispersed Phase in a Stirred Tank Reactor," *J. Chem. Eng. Japan*, **2**, 208 (1969).

Komasawa, I., et al., "A Method for Measurement of Interaction Rates of Dispersed Phase in a Continuous Flow Stirred Tank," *J. Chem. Eng. Japan*, **4**, 319 (1971).

Larson, M. A., et al., "Growth Rate Dispersion in MSMPR Crystallizers," AIChE Ann. Meet., Los Angeles (1982).

Lei, S. J., R. Shinnar, and S. Katz, "The Stability and Dynamics of a Continuous Crystallizer with Fines Trap," *AIChE J.*, **17**, 1,459 (1971a).

———, "Feedback Control of a Continuous Crystallizer with and without Fines Trap," *Chem. Eng. Prog. Symp. Ser.* No. 110, **67**, 129 (1971b).

Liao, P. F., and H. M. Hulburt, "Agglomeration Process in Suspension Crystallization," AIChE Ann. Meet., Chicago (Dec., 1976).

Lieb, E. B., "Perfect Mixing Approximation of Imperfectly Mixed Continuous Crystallizers," *AIChE J.*, **19**(3), 646 (1973).

Liss, B., and R. Shinnar, "The Dynamic Behavior of Continuous Crystallizers in which Nucleation and Growth Depend on Properties of Crystal Magma," *AIChE Symp. Ser.* No. 153, **72**, 28 (1976).

Liu, Y. A., "On the Crystal Size Intensity Function and Interpreting Population Density Data from Crystallizers," *AIChE J.*, **19**(6), 1,254 (1973).

Mao, K. W., and H. L. Toor, "A Diffusion Model for Reactions with Turbulent Mixing," *AIChE J.*, **16**, 49 (1970).

Marconi, P. F., and N. Vatistas, "Degree of Segregation and Coalescence Rate Parameter in the Random Coalescence Model for a Stirred Reactor," *AIChE J.*, **29**(3), 513 (1983).

Maruscak, A., C. G. J. Baker, and M. A. Bergougnou, "Calcium Carbonate Precipitation in a Continuous Stirred Tank Reactor," *Can. J. Chem. Eng.*, **49**, 819 (1971).

Matusevich, L. N., "Der Ein flu β von Ubersattigung, Temperatur und Impfkristallen auf die Kristallisation and waβargen Losungen," *Kristall und Technik*, **1**, 611 (1966).

McCabe, W. L., "Crystal Growth in Aqueous Solutions," *Ind. Eng. Chem.*, **21**, 112 (1929).

Mehta, R. V., and J. M. Tarbell, "Four-environment Model of Mixing and Chemical Reaction. I: Model Development," *AIChE J.*, **29**(2), 320 (1983).

Methot, J. C., and P. H. Roy, "Segregation Effects on Homogeneous Second-order Chemical Reactions," *Chem. Eng. Sci.*, **26**, 569 (1971).

Miller, P., and W. C. Saeman, "Continuous Vacuum Crystallization of Ammonium Nitrate," *Chem. Eng. Prog.*, **63**(12), 667 (1947).

Misztal, S., A. Kolek, and R. Koch, "Isotopic-Method for Studying the Kinetics of Crystal Growth," *Kristall und Technik*, **15**(11), 1,261 (1980).

Miyawaki, O., H. Tsujikawa, and Y. Urguchi, "Chemical Reactions under Incomplete Mixing," *J. Chem. Eng. Japan*, **8**, 63 (1975).

Mullin, J. W., and J. Nyvlt, "The Periodic Behavior of Continuous Crystallizers," *Chem. Eng. Sci.*, **25**, 131 (1970).

Murray, D. C., and M. A. Larson, "Size Distribution Dynamics in a Salting-out Crystallizer," *AIChE J.*, **11**, 728 (1965).

Nabholz, F., R. J. Ott, and P. Rys, "Mixing-Disguised Chemical Selectivity," *Proc. 2nd Eur. Conf. Mixing 1977*, Paper B2, BHRA, Cranfield, England, 27 (1977).

Naor, P., and R. Shinnar, "Representation and Evaluation of Residence Time Distributions," *Ind. Eng. Chem. Fundam.*, **2**, 278 (1963).

Nauman, E. B., "The Droplet Diffusion Model for Micromixing," *Chem. Eng. Sci.*, **30**, 1,135 (1975).

Nauman, E. B., and B. A. Buffham, "Mixing in Continuous Flow Systems," John Wiley, New York (1983).

Ng, D. Y. C., and D. W. T. Rippin, "The Effect of Incomplete Mixing on Conversion in Homogeneous Reactions," *Proc. 3rd Eur. Symp. Chem. Reaction Eng.*, Amsterdam, Sept. 1964, Pergamon P., Oxford, 161 (1965).

Nishimura, Y., and M. Matsubara, "Micromixing Theory via the Two-environment Model," *Chem. Eng. Sci.*, **25**, 1,785 (1970).

Nyvlt, J., "Über Kristallisation. XXII: Durchmischter Kristallisator mit Klassifikation des Produkts," *Coll. Czech. Chem. Commun.*, **32**, 903 (1967).

———, "Crystallization as a Unit Operation in Chemical Engineering," *Symp. on Indust. Crystallization*, Int. Chem. Eng., London, **1** (1969).

———, *Industrial Crystallization from Solutions*, Butterworths, London (1971).

Nyvlt, J., and M. Broul, "Crystallization Using Recycle of Mother Liquor," *Int. Chem. Eng.*, **19** (3), 547 (1979).

Nyvlt, J., and M. Karel, "Crystal Agglomeration," *Crystal Res. Tech.*, **20**, 174 (1985).

Nyvlt, J., F. Moudry, and V. Veverka, "Mathematical Models of a Cascade of Ideally Agitated Crystallizers," *Coll. Czech. Chem. Commun.*, **38**, 1,815 (1973).

Nyvlt, J., and J. W. Mullin, "Design of Classifying Crystallizers," *Trans. ICE*, **48**, 8 (1970).

Nyvlt, J., and L. Provaznik, "Optimization of Multichamber Crystallizer," *Coll. Czech. Chem. Commun.*, **44**, 1,239 (1979).

Nyvlt, J., J. Skrivanek, and F. Moudry, "Über Kristallisation. XIV: Kristallisatoren Kaskade mit Keimbildung in Allen Griedern j Reale Krystallisatoren," *Coll. Czech. Chem. Commun.*, **30**, 1,759 (1965).

Ottino, J. M., "Lamellar Mixing Models for Structured Chemical Reactions and Their Relationship to Statistical Models; Macro- and Micromixing and the Problem of Averages," *Chem. Eng. Sci.*, **35**, 1,377 (1980).

Ottino, J. M., and R. Chella, "Modeling of Rapidly Mixed Fast Crosslinking Exothermic Polymerizations," *AIChE J.*, **29**, 373 (1983).

———, "Conversion and Selectivity Modifications Due to Mixing in Unpremixed Reactors," *Chem. Eng. Sci.*, **39**(3), 551 (1984).

Ottino, J. M., W. E. Ranz, and C. W. Macosko, "A Lamellar Model for Analysis of Liquid-Liquid Mixing," *Chem. Eng. Sci.*, **34**, 877 (1979).

Ou, J., C. Lee, and S. Chen, "Mixing of Chemically Reactive Fluids by Swirling in a Tubular Reactor," *Chem. Eng. Sci.*, **38**(8), 1,323 (1983).

Ou, J., and W. E. Ranz, "Mixing and Chemical Reactions: A Contrast between Fast and Slow Reactions," *Chem. Eng. Sci.*, **38**(7), 1,005 (1983a).

———, "Mixing and Chemical Reactions: Chemical Selectivities," *Chem. Eng. Sci* **38**(7), 1,015 (1983b).

———, "Mixing and Chemical Reaction: Thermal Effects," *Chem. Eng. Sci.*, **39**(12), 1,735 (1984).

Patterson, G. K., "Simulating Turbulent Field Mixers and Reactors, or: Taking the Art of Design," in *Turbulence in Mixing Operations*, R. S. Brodkey, Ed., Academic Pr., New York, 1,221 (1975).

Petenate, A. M., and C. E. Glatz, "Isoelectric Precipitation of Soy Protein. I: Factors Affecting Particle Size Distribution," *Biotech. and Bioeng.*, **25**, 3,049 (1983a).

———, "Isoelectric Precipitation of Soy Protein. II: Kinetics of Protein Aggregate Growth and Breakage," *Biotech. and Bioeng.*, **25**, 3,059 (1983b).

Plassari, E., R. David, and J. Villermaux, "Micromixing Phenomena in Continuous Stirred Reactors Using a Michaelis-Menten Reaction in Liquid Phase," *ACS Symp. Ser.*, **65**, Chem. React. Eng., Houston, 125 (1978).

Pohorecki, R., and J. Baldyga, "New Model of Micromixing in Chemical Reactors. 1: General Development and Application to a Tubular Reactor," *Ind. Eng. Chem. Fundam.*, **22**, 392 (1983a).

———, "New Model of Micromixing in Chemical Reactors. 2: Application to a Stirred Tank Reactor," *Ind. Eng. Chem. Fundam.*, **22**, 398 (1983b).

———, "The Use of a New Model of Micromixing for Determination of Crystal Size in Precipitation," *Chem. Eng. Sci.*, **38**(1), 79 (1983c).

Ramshaw, C., and I. Parker, "Crystallizer Design Models of Steady State Operation," *Trans. ICE*, **51**(2), 82 (1973).

Randolph, A. D., "Size Distribution Dynamics in a Mixed Suspension," Ph.D. Thesis, Iowa State Univ., Ames (1962).

———, "The Mixed-Suspension, Mixed-Product Removal Crystallizer as a Concept in Crystallizer Design," *AIChE J.*, **11**, 423 (1965).

———, "Effect of Crystal Breakage on Crystal Size Distribution in a Mixed Suspension Crystallizer," *Ind. Eng. Chem. Fundam.*, **8**, 58 (1969).

———, "A Perspective on Population Models for Crystal Size Distribution," in *Industrial Crystallization 78*, E. J. de Jong and S. J. Jancic, Eds., North Holland, Amsterdam, 295 (1979).

———, "CSD Dynamics, Stability, and Control: A Review Paper," *AIChE Symp. Ser.* No. 193, **76**, 1 (1980).

Randolph, A. D., J. R. Beckman, and Z. Kraljvich, "Crystal Size Distribution Dynamics in a Classified Crystallizer: I: Experimental and Theoretical Study of Cycling in a Potassium Chloride Crystallizer," *AIChE J.*, **23**(4), 500 (1977).

Randolph, A. D., and J. R. Beckman, "Crystal Size Distribution Dynamics in a Classified Crystallizer. II: Simulated Control of Crystal Size Distribution," *AIChE J.*, **23**(4), 510 (1977).

Randolph, A. D., G. L. Beer, and J. P. Keener, "Stability of the Class II Classified Product Removal," *AIChE J.*, **19**, 1,140 (1973).

Randolph, A. D., C. Deepak, and M. Iskander, "On the Narrowing of Particle Size Distributions in Staged Vessels with Classified Product Removal," *AIChE J.*, **11**, 424 (1965).

Randolph, A. D., and Z. I. Kraljevich, "A Design-Oriented Model of Fines Dissolving," *AIChE J.*, **24**, 598 (1978).

Randolph, A. D., and M. A. Larson, "Size Distribution Analysis in Continuous Crystallization," *Chem. Eng. Prog. Symp. Ser.*, No. 95, **65**, 1 (1969).

———, "Transient and Steady State Size Distribution in Continuous Mixed Suspension Crystallizer," *AIChE J.*, **8**, 639 (1962).

———, "Analog Simulation of Dynamic Behavior in a Mixed Crystal Suspension," *Chem. Eng. Prog. Symp. Ser.* No. 55, **61**, 147 (1965).

———, "Theory of Particulate Processes," Academic Pr., New York (1971).

Randolph, A. D., C. C. Low, and E. T. White, "On-line Measurement of Fine Crystal Response to Crystallizer Disturbances," *Ind. Eng. Chem. Process Des. Dev.*, **20**, 496 (1981).

Randolph, A. D., and C. C. Low, "Some Attempts at CSD Control Utilizing On-line Measurement of Nucleation Rate," in *Industrial Crystallization 81*, S. J. Jancic and E. J. de Jong, Eds., North Holland, Amsterdam, 29 (1982).

Randolph, A. D., and T. Rivera, "A Model for the Precipitation of Pentaerythritol Tetranitrate (PETN)," *Ind. Eng. Chem. Process. Des. Dev.*, **17**(2), 182 (1978).

Randolph, A. D., and R. D. Rowang, "On-line Particle Size Analysis in the Fines Loop of a KCl Crystallizer," *AIChE Symp. Ser.* No. 193, **76**, 18 (1980).

Randolph, A. D., and C. Tan, "Numerical Design Techniques for Staged Classified Recycle Crystallizers," *Ind. Eng. Chem. Process Des. Dev.*, **17**(2), 189 (1979).

Randolph, A. D., and E. T. White, "Modeling Size Dispersion in the Prediction of Crystal Size Distribution," *Chem. Eng. Sci.*, **32**, 1,067 (1977).

Ranz, W. E., "Application of a Stretch Model to Mixing, Diffusion, and Reaction in Laminar and Turbulent Flows," *AIChE J.*, **25**, 41 (1979).

Rao, D. P., and I. J. Dunn, "A Monte Carlo Coalescence Model for Reaction with Dispersion in a Tubular Reactor," *Chem. Eng. Sci.*, **25**, 1,275 (1970).

Rao, D. P., and L. L. Edwards, "On the Diffusion Model of Mao and Toor," *AIChE J.*, **17**, 1,264 (1971).

———, "Mixing Effects in Stirred Tank Reactors: A Comparison of Models," *Chem. Eng. Sci.*, **28**, 1,179 (1973).

Remillard, M., L. Cloutier, and J. C. Methot, "Crystallisation du trihydrate d'alumine: un modele pour l'attrition," *Can. J. Chem. Eng.*, **56**, 230 (1978).

———, "Crystallisation du trihydrate d'alumine: effet des conditions d'agitation," *Can. J. Chem. Eng.*, **58**, 348 (1980).

Rice, A. W., H. L. Toor, and F. S. Manning, "Scale of Mixing in a Stirred Vessel," *AIChE J.*, **10**, 125 (1964).

Ring, T. A., "Continuous Precipitation of Monosized Particles with a Packed Bed Crystallizer," *Chem. Eng. Sci.*, **39**(12), 1,731 (1984).

Rippin, D. W. T., "Segregation in a Two-Environment Model of a Partially Mixed Chemical Reactor," *Chem. Eng. Sci.*, **22**, 247 (1967a).

———, "The Recycle Reactor as a Model of Incomplete Mixing," *Ind. Eng. Chem. Fundam.*, **6**, 488 (1967b).

Ritchie, B. W., "Simulating the Effect of Mixing on the Performance of Unpremixed Flow Chemical Reactors," *Can. J. Chem. Eng.*, **58**, 626 (1980).

Ritchie, B. W., and A. H. Tobgy, "General Population Balance Modeling of Unpremixed Feed Stream Chemical Reactors: A Review," *Chem. Eng. Commun.*, **2**, 249 (1978).

———, "A Three-Environment Micromixing Model for Chemical Reactors with Arbitrary Separate Feed Streams," *Chem. Eng. J.*, **17**, 173 (1979).

Roberts, J. E., and J. N. Robinson, "A Mathematical Study of Crystal Growth in a Cascade of Agitators," *Can. J. Chem. Eng.*, **35**, 105 (1957).

Rojkowski, Z., "Crystal Size Distribution from Cascade of Mixed Tanks," *Kristall und Technik*, **12**(11), 1,121 (1977).

Rosen, H. N., and H. M. Hulbert, "Continuous Vacuum Crystallization of Potassium Sulfate," *Chem. Eng. Prog. Symp. Ser.* No. 110, **67**, 19 (1971).

Rousseau, R. W., and T. R. Howell, "Comparison of Simulated Crystal Size Distribution Control Systems Based on Nuclei Density and Supersaturation," *Ind. Eng. Chem. Process Des. Dev.*, **21**, 606 (1982).

Saeman, W. C., "Crystal Size Distribution in Mixed Suspension," *AIChE J.*, **2**, 107 (1956).

———, "Crystallization Equipment Design," *Ind. Eng. Chem.*, **53**, 612 (1961).

Sakamoto, K., M. Kanahara, and K. Matshita, "Agglomeration Phenomenon with Crystallization," *Kagaku Kogaku*, **35**(4), 481 (1971).

Schubert, H., "Principles of Agglomeration," *Int. Chem. Eng.*, **21**(3), 363 (1981).

Seinfeld, J. H., and L. Lapidus, *Mathematical Models in Chemical Engineering*, **3**, Prentice Hall, Englewood Cliffs, NJ (1974).

Shah, Y. T., *Gass-Liquid-Solid Reactor Design*, McGraw Hill, New York, 60 (1979).

Shah, M. B., and J. Garside, "Crystallization Kinetics from MSMPR Crystallizers," *Ind. Eng. Chem. Process Des. Dev.*, **10**, 509 (1980).

Shain, S. A., "Performance of Stirred Reactors with Dispersed-phase Mixing," *AIChE J.*, **12**, 806 (1961).

Sherwin, B. M., R. Shinnar, and S. Katz, "Dynamic Behavior of the Well-Mixed Isothermal Crystallizer," *AIChE J.*, **13**(6), 1,141 (1967).

———, "Dynamic Behavior of Isothermal Well-stirred Crystallizer with Classified Outlet," *Chem. Eng. Prog. Symp. Ser.* No. 95, **65**, 75 (1969).

Shields, J. P., "Transient Behavior in Crystallization Design Models Related to Plant Experiences," in *Industrial Crystallization*, J. W. Mullin, Ed., Plenum Press, New York, 375 (1976).

Skrivanek, J., F. Moudry, and J. Nyvlt, "Über kristallisation. XX: Verteilung der teilchengrössen in einem realen kristallisator," *Coll. Czech. Chem. Eng. Commun.*, **32**, 480 (1967).

Skrivanek, J., and V. Vacek, "Crystallization in a Cascade of Ideally Stirred Vessels. Analytical Description of Moments of Distribution Function of Particle Sizes of the Crystalline Suspension," *Coll. Czech. Chem. Commun.*, **42**, 3,144 (1977).

Smoluchowski, M. V., "Three Lectures on Diffusion, Brownian Movement, and Coagulation of Colloidal Particles," *Physik. Z.*, **17**, 585 (1916).

———, "Mathematical Theory of Kinetics of the Coagulation of Colloidal Solutions," *Z. Physik. Chem.*, **92**, 129 (1917).

Song, Y., and J. M. Douglas, "Self-generated Oscillations in Continuous Crystallizer. II: An Experimental Study of an Isothermal System," *AIChE J.*, **21**, 924 (1975).

Spielman, L. A., and O. Levenspiel, "A Monte Carlo Treatment for Reacting and Coalescing Dispersed-phase Systems," *Chem. Eng. Sci.*, **20**, 247 (1965).

Szabo, T. T., and E. B. Nauman, "Copolymerization and Terpolymerisation in Continuous Nonideal Reactors," *AIChE J.*, **15**, 575 (1969).

Takao, M. and Y. Murakami, "Evaluation of Intensity of Segregation of Two-Environment Model for Micromixing," *J. Chem. Eng. Japan*, **9**, 336 (1976).

Tavare, N. S., "Studies in Crystallization," Ph.D.(Tech) Thesis, Univ. of Bombay (1978).

———, "Crystal Growth Rate Dispersion," *Can. J. Chem. Eng.*, **63**(3), 436 (1985).

———, "Micromixing Limits in an MSMPR Crystallizer," Submitted for pub. in the *Chem. Eng. J.* (1985b).

Tavare, N. S., and M. R. Chivate, "CSD Analysis from a Single-stage and Two-stage Cascade of MSCPR Crystallizers," *Can. J. Chem. Eng.*, **56**, 758 (1978).

———, "Growth and Dissolution Kinetics of Potassium Sulfate Crystals in a Fluidized Bed Crystallizer," *Trans. ICE*, **57**, 35 (1979).

———, "CSD Analysis from a Cascade of MSMPR Crystallizers," *Indian Chem. Eng.*, **24**(2), T27 (1982).

Tavare, N. S., and J. Garside, "The Characterization of Growth Dispersion," in *Industrial Crystallization 1981*, S. J. Jancic and E. J. de Jong, Eds., North Holland, Amsterdam, 21 (1982a).

———, "Estimation of Crystal Growth and Dispersion Parameters Using Pulse Response Techniques in Batch Crystallizers," *Trans. ICE*, **60**(6), 334 (1982b).

———, "Determination of the Peclet Number for Crystal Growth," *Chem. Eng. J.*, **25**(2), 229 (1982c).

———, "Multiplicity in Continuous MSMPR Crystallizers. I: Concentration Multiplicity in an Isothermal Crystallizer," *AIChE J.*, **31**(7), 1,121 (1985).

Tavare, N. S., J. Garside, and K. Akoglu, "Multiplicity in Continuous MSMPR Crystallizers. II: Temperature Multiplicity in a Cooling Crystallizer," *AIChE J.*, **31**(7), 1,128 (1985a).

Tavare, N. S., J. Garside, and M. A. Larson, "CSD Analysis from a Cascade of MSMPR Crystallizers with Magma Recycle," submitted for publication in *Chem. Eng. Commun.* (1985b).

Tavare, N. S., M. B. Shah, and J. Garside, "Crystallization and Agglomeration Kinetics of Nickel Ammonium Sulfate in an MSMPR Crystallizer," *Powder Technol.* **44**(1), 13 (1985c).

Terwillinger, J. P., and J. S. Wey, "Design Considerations for a Multistage Cascade Crystallizer," *Ind. Eng. Chem. Process Des. Dev.*, **15**, 467 (1976).

Timm, D. C., and M. A. Larson, "Effects of Nucleation Kinetics on the Dynamic Behavior of a Continuous Crystallizer," *AIChE J.*, **14**, 452 (1968).

Treleaven, C. R., and A. H. Tobgy, "Conversion in Reactors Having Separate Reactant Feed Streams. The State of Maximum Mixedness," *Chem. Eng. Sci.*, **26**, 1,259 (1971).

———, "Monte Carlo Methods of Simulating Micromixing in Chemical Reactors," *Chem. Eng. Sci.*, **27**, 1,497 (1972).

Troung, K. T., and J. C. Methot, "Segregation Effects on Consecutive Reaction in a CSTR," *Can. J. Chem. Eng.*, **54**, 572 (1976).

Tsai, B. I., et al., "The Reversed Two-environment Model of Micromixing and Growth Processes," *J. Appl. Chem. Biotechnol.*, **21**, 307 (1971).

Twineham, M., M. Hoare, and D. J. Bell, "The Effects of Protein Concentration on the Break-up of Protein Precipitate by Exposure to Shear," *Chem. Eng. Sci.*, **39**(3), 509 (1984).

Valderrama, J. O., and A. L. Gordon, "Mixing Effects on Homogeneous *p*-Order Reactors. A Two-parameter Model for Partial Segregation," *Chem. Eng. Sci.*, **34**, 1,097 (1979).

———, "A Two-parameter Model for Partial Segregation: Application to Flow Reactors with Pre- and Unmixed Feed," *Chem. Eng. Sci.*, **36**, 839 (1981).

Villermaux, J., "Drop Break-up and Coalescence. Micromixing Effects in Liquid-Liquid Reactors," in *Multiphase Chemical Reactors*, **I**, Rodrigues, Calo, and Sweed, Eds., Nato Adv. Study Inst., Series E., Appl. Sci., **52**, Sijthoff Noordhoff (1981).

Villermaux, J., and R. David, "Recent Advances in the Understanding of Micromixing Phenomena in Stirred Reactors," *Chem. Eng. Commun.*, **21**, 105 (1983).

Villermaux, J., and A. Zoulalian, "Etat de Melange du Fluide dans un Reacteur Continu. A Propos d'un Modele de Weinstein et Alder," *Chem. Eng. Sci.*, **24**, 1,513 (1969).

Wahl, E. F., and C. G. J. Baker, "The Kinetics of Titanium Dioxide Agglomeration in an Agitated Liquid Suspension," *Can. J. Chem. Eng.*, **49**, 742 (1971).

Walton, A. G., *The Formation and Properties of Precipitates*, Interscience, New York (1967).

Weinstein, H. J., and R. J. Alder, "Micromixing Effects in Continuous Chemical Reactors," *Chem. Eng. Sci.*, **22**, 65 (1967).

Wen, C. Y., and L. T. Fan, *Models for Flow Systems and Chemical Reactors*, Dekker, New York (1975).

White, E. T., L. L. Bendig, and M. A. Larson, "The Effect of Size on the Growth Rates of Potassium Sulfate Crystals," *Chem. Eng. Prog. Symp. Ser.* No. 110, **67**, 97 (1971).

Wolff, P. R., and M. A. Larson, "Crystal Size Distributions from Multistage Crystallizers," *Chem. Eng. Prog. Symp. Ser.*, No. 110, **67**, 97 (1971).

Yu, K. M., and J. M. Douglas, "Self-generated Oscillations in Continuous Crystallizers. I: Analytical Prediction of the Oscillating Output," *AIChE J.*, **21**(5), 917 (1975).

Zacek, S., et al., "A Stirred Tank for Continuous Crystallization Studies," *Chem. Eng. J.*, **23**, 111 (1982).

Zeitlin, M. A., and L. L. Tavlarides, "Fluid-Fluid Interactions and Hydrodynamics in Agitated Dispersion," *Can. J. Chem. Eng.*, **50**, 207 (1972).

Zoulalian, A., and J. Villermaux, "Influence of Chemical Parameters on Micromixing in a Continuous Stirred Tank Reactor," *Adv. Chem. Ser.* Am. Chem. Soc., **133**, 348 (1974).

Zwietering, T. N., "The Degree of Mixing in Continuous Flow Systems," *Chem. Eng. Sci.*, **11**, 1 (1959).

———, "Suspending of Solid Particles in Liquid by Agitators," *Chem. Eng. Sci.*, **8**, 244 (1958).

Manuscript received Apr. 8, 1985, and revision received July 22, 1985.